anti-apoptotic effects on *Abca12*$^{-/-}$ keratinocytes, we performed TUNEL staining of keratinocytes treated with AKT inhibitor, which blocks AKT phosphorylation (#124017; InSolution Akt Inhibitor VIII, Calbiochem, San Diego, CA). *Abca12*$^{-/-}$ keratinocytes incubated with 10 μM #124017 AKT inhibitor showed a notably greater number of TUNEL-positive cells than both wild-type keratinocytes with AKT inhibitor and *Abca12*$^{-/-}$ keratinocytes without AKT inhibitor (Figure 2). These results suggest that AKT activation helps *Abca12*$^{-/-}$ keratinocytes to avoid apoptosis. Furthermore, mRNA and protein levels of peroxisome proliferator-activated receptor (PPAR)-δ from *Abca12*$^{-/-}$ epidermis were shown to be significantly higher than those from wild-type epidermis (Taqman Gene Expression Assay, probe ID, Mm00803184_m1, Mm99999915_g1, Applied Biosystems, Carlsbad, CA; anti-PPAR-δ antibody H-74, Santa Cruz, Santa Cruz, CA; Supplementary Figure S1 online), which suggests upregulation of PPAR-δ as a candidate pathway for AKT activation.

Herein, we have suggested that apoptosis is involved in the pathomechanism of HI. Defective lipid transport due to loss of ABCA12 function leads to the accumulation of intracellular lipids, including glucosylceramides and gangliosides (Akiyama *et al.*, 2005; Mitsutake *et al.*, 2010). Studies by Wang *et al.* (2001) and Sun *et al.* (2002) showed that the elevation of ganglioside levels leads to keratinocyte apoptosis. Thus, we are able to speculate that the accumulation of gangliosides leads to the apoptosis of *Abca12*$^{-/-}$ keratinocytes, although the exact mechanism of apoptosis in *Abca12*$^{-/-}$ keratinocytes remains unclear.

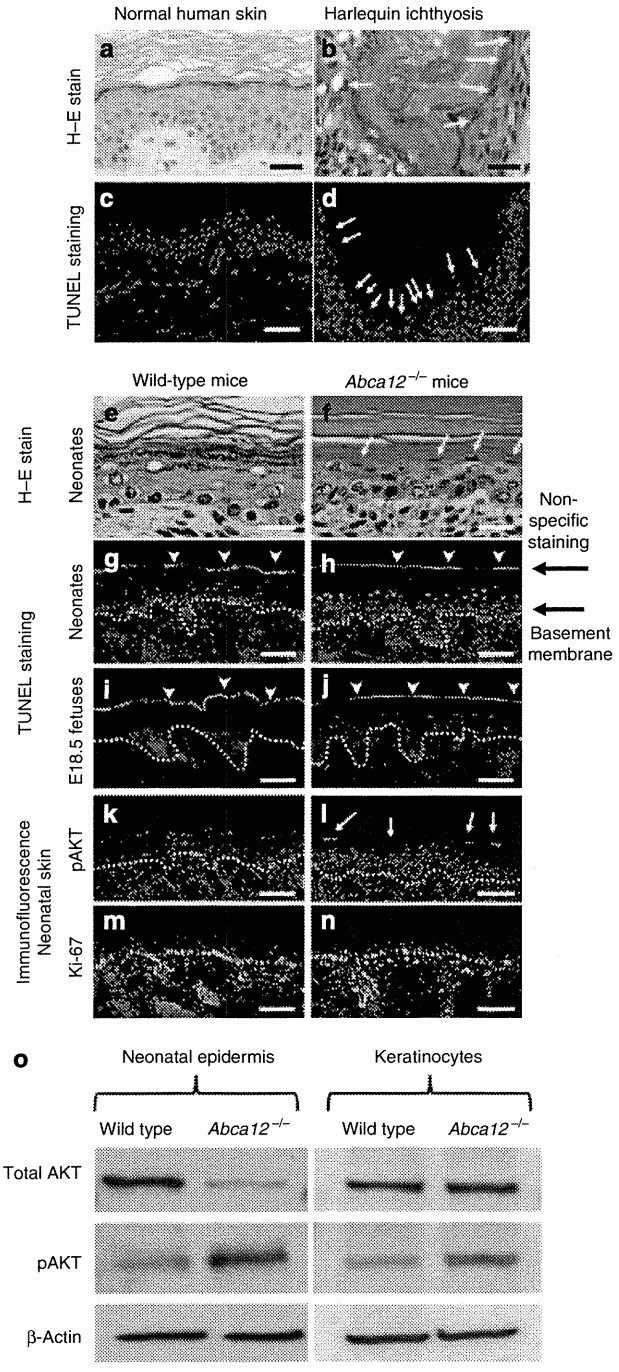

Figure 1. ATP-binding cassette transporter A12-deficient keratinocytes show TUNEL-positive nuclei and AKT activation. (**a–d**) In the harlequin ichthyosis patients, the nuclei of the granular-layer keratinocytes are condensed (**b**, white arrows) and they show positive TUNEL labeling (**d**, white arrows), although apoptotic nuclei are rare in the normal human epidermis (**a**, **c**). Data shown are representative of those from the two harlequin ichthyosis patients. (**e**, **f**) Granular-layer keratinocytes of *Abca12*$^{-/-}$ mice show more condensed nuclei (**f**, white arrows) than those of wild-type mice (**e**). (**g–j**) Granular-layer keratinocytes of *Abca12*$^{-/-}$ mice, a neonate (**h**) and an 18.5-day embryo (**j**), show TUNEL-positive nuclei. No TUNEL-positive cells are seen in the epidermis of the control wild-type mice (**g**, **i**). Dotted lines indicate the basement membrane. Nonspecific staining is seen on the skin surface (white arrowheads). (**k**, **l**) By immunofluorescence staining, AKT activation (Ser-473 phosphorylated AKT; green) is observed in granular-layer keratinocytes of *Abca12*$^{-/-}$ mice. (**m**, **n**) Immunofluorescence staining for the Ki-67-proliferation marker shows similar staining patterns of basal keratinocytes in wild-type (**m**) and *Abca12*$^{-/-}$ (**n**) samples. (**a**, **b**, **e**, **f**; hematoxylin–eosin (H–E) stain. Bars of **c**, **d**, **g**, **h**, **i**, **j**, **k**, **l**, **m**, **n** = 20 μm. Bars of **a**, **b**, **e**, **f** = 5 μm.) (**o**) Immunoblot analysis shows that levels of serine-473-phosphorylated AKT (pAKT) in neonatal epidermis and differentiated keratinocytes of *Abca12*$^{-/-}$ mice are higher than those of wild-type mice.

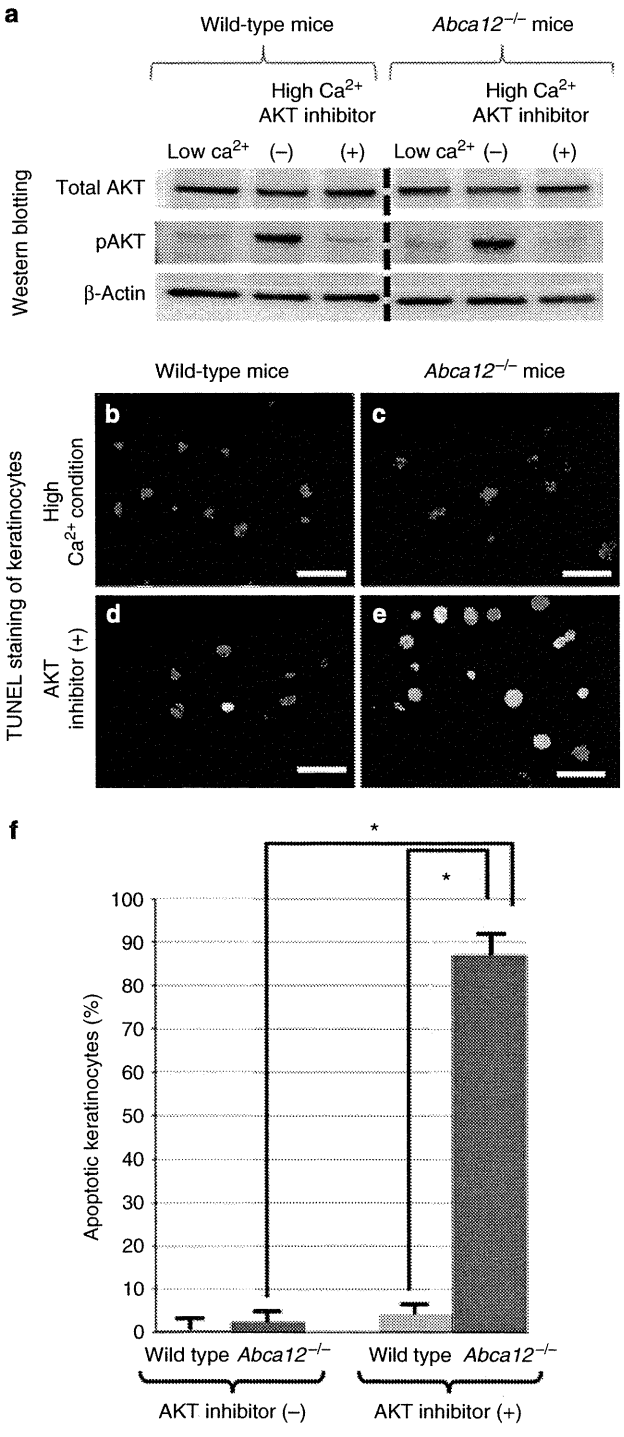

Figure 2. Inhibition of AKT activation leads to apoptosis of *Abca12*$^{-/-}$ keratinocytes. (**a**) Immunoblot analysis indicates that the AKT inhibitor can inhibit AKT activation (phosphorylated AKT (pAKT) synthesis) in differentiated keratinocytes. (**b–e**) TUNEL staining of keratinocytes cultured under high Ca^{2+} condition treated with/without the AKT inhibitor. Neither wild-type cells (**b**) nor *Abca12*$^{-/-}$ cells (**c**) are TUNEL positive. *Abca12*$^{-/-}$ keratinocytes with the AKT inhibitor (#124017; 10 μM) show many TUNEL-positive nuclei (**e**), although only a small number of wild-type cells with the AKT inhibitor are TUNEL positive (**d**). (Bars = 20 μm.) (**f**) Percentage of TUNEL-positive keratinocytes. *Abca12*$^{-/-}$ keratinocytes with AKT inhibitor shows a significantly greater number of TUNEL-positive nuclei than wild-type keratinocytes with/without the AKT inhibitor and *Abca12*$^{-/-}$ keratinocytes without the AKT inhibitor. ($n = 3$, mean ± SD, $^*P < 0.05$).

Although *Abca12*$^{-/-}$ granular-layer keratinocytes show characteristics of apoptosis, including condensed nuclei and positive TUNEL labeling, they are able to form epidermal stratification. In several disorders involving keratinocyte apoptosis, e.g., toxic epidermal necrolysis, the apoptotic epidermal keratinocytes show not only TUNEL-positive nuclei but also defective epidermal stratification (Abe *et al.*, 2003). Thrash *et al.* (2006) reported that AKT1 activation is an essential signal for keratinocyte cell survival and stratification, by experiments with gene silencing and three-dimensional cell cultures. Thus, we hypothesized that the AKT pathway might work as a compensatory mechanism against apoptosis in *Abca12*$^{-/-}$ keratinocytes. We have clearly shown that AKT activation occurs in *Abca12*$^{-/-}$ granular-layer keratinocytes, which suggests that AKT activation serves to prevent the cell death of *Abca12*$^{-/-}$ keratinocytes. By immunoblot analysis using anti-AKT1/2/3 antibodies (#2938/3063/3788, Cell Signaling), *Abca12*$^{-/-}$ epidermis showed expression of AKT1 and AKT2, but not AKT3 (Supplementary Figure S2 online). Compared with wild-type epidermis, *Abca12*$^{-/-}$ epidermis seemed to have more AKT1 than AKT2. From our data and the literature (Thrash *et al.*, 2006), we are able to speculate that AKT1 is the major isoform of phosphorylated AKT in *Abca12*$^{-/-}$ epidermis.

We have shown that PPAR-δ is a candidate molecule in the upstream of the AKT activation pathway in *Abca12*$^{-/-}$ keratinocytes. Di-Poi *et al.* (2002) reported that PPAR-δ has an anti-apoptotic role in keratinocytes via transcriptional control of the AKT1 signaling pathway. PPAR-δ also regulates the expression of ABCA12 (Jiang *et al.*, 2008). From these studies, we can speculate that upregulation of PPAR-δ is in response to apoptosis or decreased ABCA12 expression. To ascertain the function of PPAR-δ, we performed the experiments using a PPAR-δ-specific antagonist (GSK0660, Santa Cruz). Differentiated *Abca12*$^{-/-}$ keratinocytes treated with 1 μM GSK0660 for 48 hours showed TUNEL-positive nuclei, from which we are able to speculate an anti-apoptotic role for

PPAR-δ in *Abca12*$^{-/-}$ keratinocytes (Supplementary Figure S1 online). From our studies and the literature (Di-Poi *et al.*, 2002), PPAR-δ has been shown to have at least an anti-apoptotic role in *Abca12*$^{-/-}$ keratinocytes; however, it remains unclear whether the upregulation of PPAR-δ is in response to apoptosis or decreased ABCA12 expression.

Furthermore, we have measured the mRNA expression levels of other nuclear hormone receptors, including PPAR-α, PPAR-γ, retinoic acid receptor-α, liver X receptor-α, liver X receptor-β, RXR-α, and RXR-γ (Applied Biosystems). The mRNA level of RXR-α from *Abca12*$^{-/-}$ epidermis was shown to be significantly higher than that from wild-type epidermis (Supplementary Figure S1 online). The interaction between the upregulation of RXR-α and AKT activation in keratinocytes has not been reported. However, Wang *et al.* (2011) reported that RXR-α ablation in the epidermis enhances UV-induced apoptosis, which suggests that RXR-α has an anti-apoptotic function in keratinocytes. Thus, upregulation of RXR-α may also have an anti-apoptotic function in *Abca12*$^{-/-}$ keratinocytes.

In conclusion, the present data suggest that keratinocyte apoptosis is involved in the pathomechanisms of HI and that the AKT signaling pathway helps *Abca12*$^{-/-}$ keratinocytes to survive during the keratinization process. In light of this, activation of the AKT signal pathway may be to our knowledge, previously unreported strategy for treating keratinization disorders, including ichthyosis.

CONFLICT OF INTEREST

The authors state no conflict of interest.

ACKNOWLEDGMENTS

We thank Ms Aoyanagi for her technical assistance. This work was supported in part by a grant-in-aid from the Ministry of Education, Science, Sports and Culture of Japan (Kiban A 23249058: to MA), a grant from the Ministry of Health, Labor and Welfare of Japan (Health and Labor Sciences Research Grants; Research on Intractable Disease: H22-177: to MA), and a grant-in-aid from the Japan Society for the Promotion of Science Fellows (to TY).

***Teruki Yanagi*[1], *Masashi Akiyama*[1,2], *Hiroshi Nishihara*[3], *Yuki Miyamura*[1], *Kaori Sakai*[1], *Shinya Tanaka*[4] and *Hiroshi Shimizu*[1]**

[1]Department of Dermatology, Hokkaido University Graduate School of Medicine, Sapporo, Japan; [2]Department of Dermatology, Nagoya University Graduate School of Medicine, Nagoya, Japan; [3]Laboratory of Translational Pathology, Hokkaido University Graduate School of Medicine, Sapporo, Japan and [4]Laboratory of Cancer Research, Department of Pathology, Hokkaido University Graduate School of Medicine, Sapporo, Japan
E-mail: makiyama@med.nagoya-u.ac.jp

SUPPLEMENTARY MATERIAL

Supplementary material is linked to the online version of the paper at http://www.nature.com/jid

REFERENCES

Abe R, Shimizu T, Shibaki A *et al.* (2003) Toxic epidermal necrolysis and Stevens-Johnson syndrome are induced by soluble Fas ligand. *Am J Pathol* 162:1515–20

Akiyama M, Sugiyama-Nakagiri Y, Sakai K *et al.* (2005) Mutations in lipid transporter ABCA12 in harlequin ichthyosis and functional recovery by corrective gene transfer. *J Clin Invest* 115:1777–84

Di-Poi N, Tan NS, Michalik L *et al.* (2002) Antiapoptotic role of PPARbeta in keratinocytes via transcriptional control of the Akt1 signaling pathway. *Mol Cell* 10:721–33

Jiang YJ, Lu B, Kim P *et al.* (2008) PPAR and LXR activators regulate ABCA12 expression in human keratinocytes. *J Invest Dermatol* 128:104–9

Mitsutake S, Suzuki C, Akiyama M *et al.* (2010) ABCA12 dysfunction causes a disorder in glucosylceramide accumulation during keratinocyte differentiation. *J Dermatol Sci* 60:128–9

Moskowitz DG, Fowler AJ, Heyman MB *et al.* (2004) Pathophysiologic basis for growth failure in children with ichthyosis: an evaluation of cutaneous ultrastructure, epidermal permeability barrier function, and energy expenditure. *J Pediatr* 145:82–92

Sun P, Wang XQ, Lopatka K *et al.* (2002) Ganglioside loss promotes survival primarily by activating integrin-linked kinase/Akt without phosphoinositide 3-OH kinase signaling. *J Invest Dermatol* 119:107–17

Thrash BR, Menges CW, Pierce RH *et al.* (2006) AKT1 provides an essential survival signal required for differentiation and stratification of primary human keratinocytes. *J Biol Chem* 281:12155–62

Uchida Y, Houben E, Park K *et al.* (2010) Hydrolytic pathway protects against ceramide-induced apoptosis in keratinocytes exposed to UVB. *J Invest Dermatol* 130: 2472–80

Wang XQ, Sun P, Paller AS (2001) Inhibition of integrin-linked kinase/protein kinase B/Akt signaling: mechanism for ganglioside-induced apoptosis. *J Biol Chem* 276:44504–11

Wang Z, Coleman DJ, Bajaj G *et al.* (2011) RXRalpha ablation in epidermal keratinocytes enhances UVR-induced DNA damage, apoptosis, and proliferation of keratinocytes and melanocytes. *J Invest Dermatol* 131:177–87

Yanagi T, Akiyama M, Nishihara H *et al.* (2008) Harlequin ichthyosis model mouse reveals alveolar collapse and severe fetal skin barrier defects. *Hum Mol Genet* 17:3075–83

Yanagi T, Akiyama M, Nishihara H *et al.* (2010) Self-improvement of keratinocyte differentiation defects during skin maturation in ABCA12-deficient harlequin ichthyosis model mice. *Am J Pathol* 177:106–18

See related commentary on pg 1790

Interpretation of Skindex-29 Scores: Cutoffs for Mild, Moderate, and Severe Impairment of Health-Related Quality of Life

Journal of Investigative Dermatology (2011) **131,** 1945–1947; doi:10.1038/jid.2011.138; published online 19 May 2011

TO THE EDITOR

Health-related quality of life (HRQL) is commonly assessed by means of standardized questionnaires and expressed in domain and overall HRQL scores. An important challenge is to interpret these scores correctly. What does a given score really mean? Although there is no standard approach, several methods exist to facilitate the interpretation of HRQL scores.

In a recently published study (Prinsen *et al.*, 2010), we identified

Abbreviation: HRQL, health-related quality of life

Recurrence of Hydroxyurea-induced Leg Ulcer After Discontinuation of Treatment

Kazuhiro Kikuchi[1], Ken Arita[1], Yasuki Tateishi[1], Masahiro Onozawa[2], Masashi Akiyama[1] and Hiroshi Shimizu[1]
Departments of [1]Dermatology and [2]Hematology, Hokkaido University Graduate School of Medicine, North 15 West 7, Kita-ku, Sapporo 060-8638, Japan.
E-mail: kikku@med.hokudai.ac.jp
Accepted November 1, 2010.

Hydroxyurea (HU) is a hydroxylated derivative of urea that has been recognized since 1960 as effective against cancer (1). It is an inhibitor of cellular DNA synthesis, and it promotes cell death in the S phase of the cell cycle through inhibition of the enzyme ribonucleotide reductase (2). The most common indications for HU therapy are chronic myeloid leukaemia and other myeloproliferative disorders (3, 4) such as essential thrombocythemia (5) and polycythemia vera (PV) (6). Cutaneous side-effects, such as alopecia, diffuse hyperpigmentation, scaling, lichen planus-like lesions, poikiloderma, atrophy of the skin and subcutaneous tissues, and nail changes, can occur during the treatment with HU (7–9). The occurrence of painful leg ulcers represents another rare and incompletely characterized complication that has been described in patients with myeloproliferative diseases receiving high-dose long-term HU treatment (10). While the mode of action of HU on bone marrow elements is well established, its effects on actively proliferating epithelial cells remain less described (11). Poor response to traditional local and systemic therapy is a typical feature of HU-induced leg ulcers, and discontinuation of the drug is often required to achieve complete wound healing (6, 8). Cessation of the drug usually improves the skin ulcer; although, in some cases, the ulcer remains and additional therapies, such as skin grafting, are needed (12). We report here the first case of a leg ulcer that recurred even after discontinuation of HU treatment.

CASE REPORT

The patient was an 82-year-old Japanese male who had been diagnosed with PV 9 years before and had been treated only with phlebotomy and an anti-platelet agent for several years. Due to splenomegaly and elevated blood cell counts, HU therapy was started 3 years ago at a dosage of 1 g daily for a month, followed by 1.0 or 1.5 g daily for 28 months. A good clinical response was achieved. However, the patient developed painful ulcers on the left second toe after two years of HU treatment.

He visited our outpatient clinic and was diagnosed with an HU-induced skin ulcer. HU was discontinued, topical application of sulfadiazine silver was performed, an oral antibiotic (cefdinir) was administered, and the ulcer epithelialized. However, a new ulcer appeared on the left lateral malleolar area 46 days after cessation of HU and gradually enlarged in size. The patient was admitted to our hospital for treatment of the ulcer.

Examination revealed a 48 × 56 mm ulcer with yellow necrotic tissue and marginal erythematous oedema (Fig. 1). Laboratory examination revealed a white blood cell count of $11.6 \times 10^3/\mu l$, a platelet count of $64.2 \times 10^4/l$, and a red blood cell count of $5.07 \times 10^6/\mu l$. Anti-nuclear antibody, anti-neutrophilic cytoplasmic antibodies, anti-cardiolipin antibody, and cryoglobulin were negative. A skin biopsy taken from the margin of the ulcer demonstrated leukocytoclastic vasculitis in the upper dermis (Fig. 2). A wound-healing strategy of surgical debridement, intravenous prostaglandin E1 administration, and topical application of beta-fibroblast growth factor, sulfadiazine silver and alprostadil alfadex was started, and the ulcer began to epithelialize. After 4 months, re-epithelialization was complete. The PV was treated with busulfan, achieving a good clinical response.

DISCUSSION

HU is usually well tolerated and has low toxicity (1). However, cutaneous adverse effects such as diffuse hyperpigmentation, brown discoloration of the nails, acral erythema, photosensitization, fixed drug eruption, alopecia, and oral ulceration have been reported (7–9). Stahl & Silber (10) first reported HU-induced skin ulcers in 1985. Montefusco et al. (11) reported

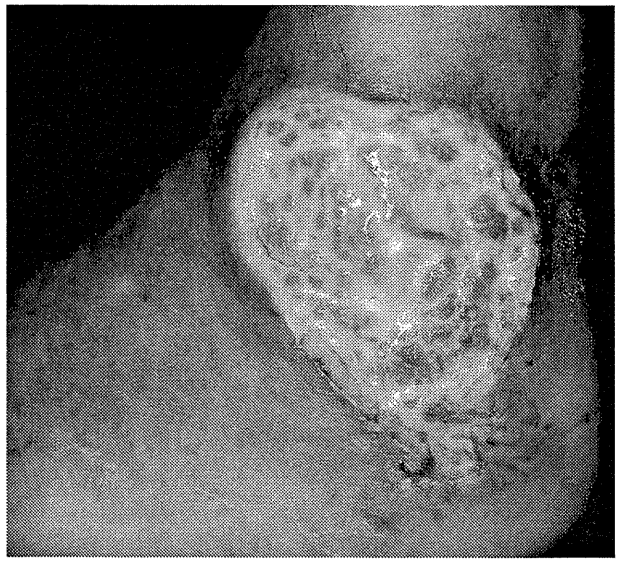

Fig. 1. Left foot with an ulcer on the lateral malleolar area after two months free of hydroxyurea administration. The ulcer was covered with yellow necrotic tissue and surrounded by oedematous erythema.

 doi: 10.2340/00015555-1048
 ISSN 0001-5555

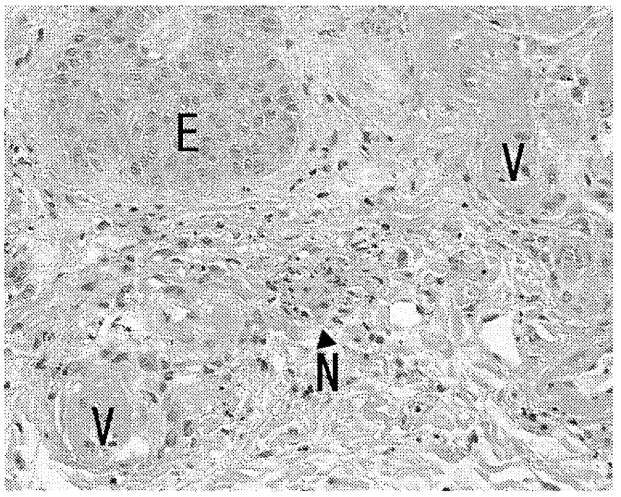

Fig. 2. Histology of erythema on the margin of the ulcer (haematoxylin-eosin staining). Fibrin deposition on the vascular wall and nucleic debris were evident around small vessels (×100). (E: epidermis; V: blood vessels; N: neutrophilic nuclear debris)

that, among 200 chronic myeloid leukaemia patients treated with HU, 17 (8.5%) developed leg ulcers. However, they achieved complete resolution or significant improvement after discontinuation of HU therapy (11). HU-induced leg ulcer and complete resolution within several months after drug discontinuation has also been reported in other myeloproliferative disorder, such as PV (6) and essential thrombocythemia (5). In those cases, as in ours, most of the patients had been treated with > 1 g of HU per day for at least one year (8). In the present case, the patient was treated with > 1 g of HU per day for 28 months. The ulcer occurred on his lateral malleolus, which histologically showed leukocytoclastic vasculitis. These features are consistent with previous reports of HU-induced leg ulcer.

From previous reports, the pathogenesis of HU-induced ulceration remains unclear and it may be multifactorial. It has been postulated that ulcers may be the result of: (*i*) interruption of microcirculation due to leukocytoclastic vasculitis or arterial microthrombi related to platelet dysregulation (13, 14); (*ii*) cumulative toxicity in the basal layer of the epidermis through inhibition of DNA synthesis (8); and (*iii*) repeated mechanical injury in areas subject to trauma: a perimalleolar area for instance (15).

In the case described here, a new ulcer developed even after cessation of HU administration. As for the pathogenic mechanism of recurrence, (*i*) interruption of microcirculation could result from hyperviscosity due to the elevated platelet count (as high as 100×10^4/l in one measurement) (13, 14), although no thrombi were observed histologically in the capillaries or small vessels. (*ii*) The direct cytotoxic effect of HU (8) may continue even after the withdrawal of the drug, and it may inhibit the repair of (*iii*) small injuries in the perimalleolar area: the one of the area susceptible to physical trauma (15). These assumptions can be made from the pathogenesis of HU-induced ulcer reported previously (8, 13–15).

To our knowledge, this is the first report of recurrence of HU-related leg ulcer after the discontinuation of medication. The case suggests that it is important to pay careful attention to recurrence even after cessation of HU therapy. Precise, early treatment for microtraumas and small ulcers should be administered to patients with a long history of HU medication.

REFERENCES

1. Boyd AS, Neldner KH. Hydroxyurea therapy. J Am Acad Dermatol 1991; 25: 518–524.
2. Yarbro JW. Mechanism of action of hydroxyurea. Semin Oncol 1992; 19: 1–10.
3. Goldman JM. Therapeutic strategies for chronic myeloid leukemia in the chronic (stable) phase. Semin Hematol 2003; 40: 10–17.
4. Rice L, Baker KR. Current management of the myeloproliferative disorders: a case-based review. Arch Pathol Lab Med 2006; 130: 1151–1156.
5. Demirçay Z, Cömert A, Adigüzel C. Leg ulcers and hydroxyurea: report of three cases with essential thrombocythemia. Int J Dermatol 2002; 41: 872–874.
6. Bader U, Banyai M, Böni R, Burg G, Hafner J. Leg ulcers in patients with myeloproliferative disorders: disease- or treatment-related? Dermatology 2000; 200: 45–48.
7. Najean Y, Rain JD. Treatment of polycythemia vera: the use of hydroxyurea and pipobroman in 292 patients under the age of 65 years. Blood 1997; 90: 3370–3377.
8. Weinlich G, Schuler G, Greil R, Kofler H, Fritsch P. Leg ulcers associated with long-term hydroxyurea therapy. J Am Acad Dermatol 1998; 39: 372–374.
9. Daoud MS, Gibson LE, Pittelkow MR. Hydroxyurea dermopathy: a unique lichenoid eruption complicating long-term therapy with hydroxyurea. J Am Acad Dermatol 1997; 36: 178–182.
10. Stahl RL, Silber R. Vasculitic leg ulcers in chronic myelogenous leukemia. Am J Hematol 1985; 78: 869–872.
11. Montefusco E, Alimena G, Gastaldi R, Carlesimo OA, Valesini G, Mandelli F. Unusual dermatologic toxicity of long-term therapy with hydroxyurea in chronic myelogenous leukaemia. Tumori 1986; 72: 317–321.
12. Kato N, Kimura K, Yasukawa K, Yoshida K. Hydroxyurea-related leg ulcers in a patient with chronic myelogenous leukemia: a case report and review of the literature. J Dermatol 1999; 26: 56–62.
13. Sirieix ME, Debure C, Baudot N, Dubertret L, Roux ME, Morel P, et al. Leg ulcers and hydroxyurea: forty-one cases. Arch Dermatol 1999; 135: 818–820.
14. Chaine B, Neonato MG, Girot R, Aractingi S. Cutaneous adverse reactions to hydroxyurea in patients with sickle cell disease. Arch Dermatol 2001; 137: 467–470.
15. Saravu K, Velappan P, Lakshmi N, Shastry BA, Thomas J. Hydroxyurea induced perimalleolar ulcers. J Korean Med Sci 2006; 21: 177–179.

International Journal of
Dermatology

Medical genetics

DNA-based prenatal diagnosis of plectin-deficient epidermolysis bullosa simplex associated with pyloric atresia

Hideki Nakamura, Ken Natsuga, MD, PhD, Wataru Nishie, MD, PhD, James R. McMillan, PhD, Hiroyuki Nakamura, MD, PhD, Daisuke Sawamura, MD, PhD, Masashi Akiyama, MD, PhD, and Hiroshi Shimizu, MD, PhD

From the Department of Dermatology, Hokkaido University Graduate School of Medicine, Sapporo, Japan

Correspondence
Dr Hiroshi Shimizu, MD, PhD
Department of Dermatology
Hokkaido University Graduate School of Medicine
North 15 West 7, Sapporo
Japan
E-mail: shimizu@med.hokudai.ac.jp

Conflicts of interest: The authors declare no conflicts of interest.

Abstract

Background Mutations in the plectin gene (*PLEC*) generally lead to epidermolysis bullosa simplex (EBS) associated with muscular dystrophy. It has been recently demonstrated that *PLEC* mutations can also cause a different clinical subtype, EBS associated with pyloric atresia (EBS-PA), which shows early lethality. Prenatal diagnosis (PND) of EBS-PA using mutation screening of *PLEC* has not been described.

Objective This study aimed to perform DNA-based PND for an EBS-PA family.

Materials and methods The EBS-PA proband was compound-heterozygous for a paternal c.1350G>A splice-site mutation and a maternal p.Q305X nonsense mutation. Genomic DNA was obtained from amniocytes taken from an at-risk fetus of the proband's family. Direct sequencing and restriction enzyme digestion of polymerase chain reaction products from the genomic DNA were performed.

Results Mutational analysis showed that the fetus harbored both pathogenic mutations, suggesting that the fetus was a compound-heterozygote and therefore affected with EBS-PA. The skin sample obtained by autopsy from the abortus confirmed the absence of plectin expression at the dermal–epidermal junction.

Conclusions This is the first successful DNA-based PND for an EBA-PA family.

Introduction

Epidermolysis bullosa (EB) comprises a group of diseases that are classified into four categories – EB simplex (EBS), junctional EB (JEB), dystrophic EB, and Kindler syndrome – depending on the depth of the dermal-epidermal junction split.[1] The four categories are subcategorized into minor subtypes, some of which show severe prognosis and lead to early demise.

Prenatal diagnosis (PND) of lethal EB subtypes has been performed for more than two decades. Electron microscopy and immunofluorescence analysis of fetal skin samples were the mainstay for PND of EB fetuses.[2] However, morphologically based PND had technical difficulties and abortion risks from the fetal skin biopsies. As the genes responsible for EB have been indentified, DNA-based PND has been available for many lethal EB subtypes.[2,3] Recently, other techniques such as immunofluorescence analysis of villous trophoblasts,[4] preimplantation genetic analysis[5], and preimplantation genetic haplotyping[6] have been described as useful for PND of EB.

Among the lethal EB subtypes, EB associated with pyloric atresia (EB-PA) has been known to result from mutations in the genes encoding either plectin (*PLEC*), or α6 (*ITGA6*), or β4 integrin (*ITGB4*).[1] EB-PA can either manifest as JEB with PA (JEB-PA) or EBS with PA (EBS-PA) and is categorized as hemidesmosomal variant of EB. EB-PA due to *ITGA6* or *ITGB4* mutations is generally characterized by blister formation at the level of the lamina lucida as JEB-PA, although skin separation within basal keratinocytes has been described in a few cases.[1] In contrast, it has been recently reported that another subset of lethal EB-PA shows an intraepidermal level of cleavage consistent with EBS, caused by mutations in the gene encoding plectin (*PLEC*).[7–9] To date, PND of EBS-PA using mutation screening of *PLEC* has not been reported in the literature. This paper describes the first DNA-based PND for an EBS-PA family.

Materials and Methods

The EBS-PA family

We previously reported this family with EBS-PA, in which the first and second newborns exhibited the clinical features of blistering and PA and died shortly after birth.[7] We then identified the precise genetic abnormality in the family through immunohistochemical analysis and genetic screening using the candidate gene approach. *PLEC* mutation analysis of genomic DNA from the parents and the proband demonstrated a paternal c.1350G>A splice-site mutation and a maternal p.Q305X nonsense mutation.[7] c.1350G>A was originally described as c.1344G>A and corrected according to the latest sequence information (GeneBank Accession No. NM_000445), plectin isoform 1c.[10] The parents were found to be heterozygous carriers, and the proband was compound-heterozygous (Fig. 1). The parents sought PND for a subsequent pregnancy.

PND

Amniocentesis was performed at 16 weeks gestation. Genomic DNA isolated from one-week-cultured amniocytes maintained in Amniomax medium (Invitrogen, Carlsbad, CA, USA) was subjected to polymerase chain reaction (PCR) amplification, followed by direct automated sequencing using an ABI Prism 3100 genetic analyser (Advanced Biotechnologies, Foster City, CA, USA). PCR amplification of the *PLEC* gene exons 9 and 12 was performed using the following primers. Primers 5′-GTCGCT GTATGACGCCATGC-3′ and 5′-TGGCTGGTAGCTCCATC TCC-3′ were used for amplification of exon 9, producing a 387-bp fragment. Primers 5′-CCCACTCGCCTTAGGACAGT-3′ and 5′-AAACCAACTCTGCCCAAAGC-3′ were used for amplification of exon 12, synthesizing a 428-bp fragment. PCR conditions were five minutes at 94 °C for one cycle, followed by 38 cycles of 45 seconds at 94 °C, 30 seconds at 57 °C or 60 °C, and one minute at 72 °C. The genomic DNA nucleotides, the cDNA nucleotides, and the amino acids of the protein were numbered based on the latest sequence information (GeneBank Accession No. NM_000445).

Written informed consent was obtained from the parents. PND was approved by the Institutional Ethical Committee of Hokkaido University Graduate School of Medicine. This study was conducted according to the Declaration of Helsinki Principles.

Immunofluorescence analysis

Immunofluorescence analysis using a series of antibodies against basement-membrane-associated molecules on cryostat skin sections was performed as previously described.[11] Skin biopsy was performed for the aborted fetus and a healthy volunteer as the normal control. The following monoclonal antibodies (mAbs) were used: mAb HD1–121 (a gift from Dr K. Owaribe of Nagoya University) against plectin; mAb GoH3 (a gift from Dr A. Sonnenberg of the Netherlands Cancer Institute) against α6 integrin; and mAb 3E1 (Chemicon, CA, USA) against β4 integrin.

Results

Mutation analysis of genomic DNA from amniocytes showed both paternal c.1350G>A splice-site mutation and maternal p.Q305X nonsense mutation (Fig. 2a). These mutation data were briefly mentioned in our recent paper on plectin expression patterns in patients with EBS.[12] Each mutation was confirmed by restriction enzyme digestion of PCR products. The c.1350G>A and p.Q305X mutations resulted in the loss of a restriction site for *Hph* I and *Pst* I, respectively (Fig. 2b). The prenatal molecular genetic diagnosis suggested that the fetus

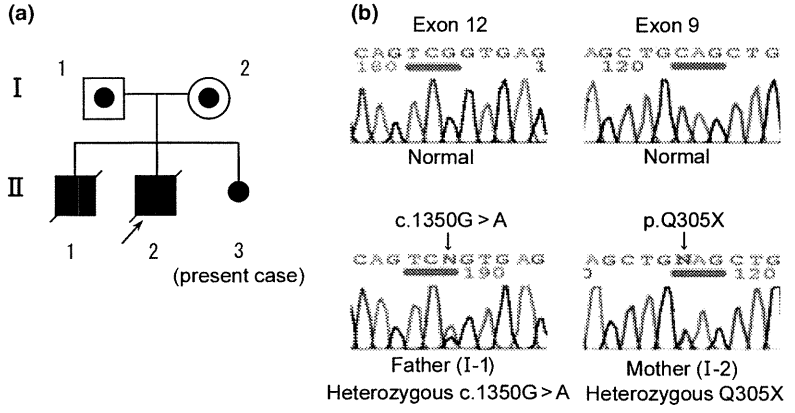

Figure 1 Family tree of the present case and the causative *PLEC* mutations. (a) The first and second newborns exhibited clinical features typical of EBS-PA and died shortly after birth. The proband (the second newborn) is indicated by an arrow. (b) The paternal splice-site mutation was a c.1350G>A transition at the end of exon 12. The maternal nonsense mutation was a c.913C>T transition in exon 9, leading to the substitution of glutamine 305 with a nonsense codon (p.Q305X)

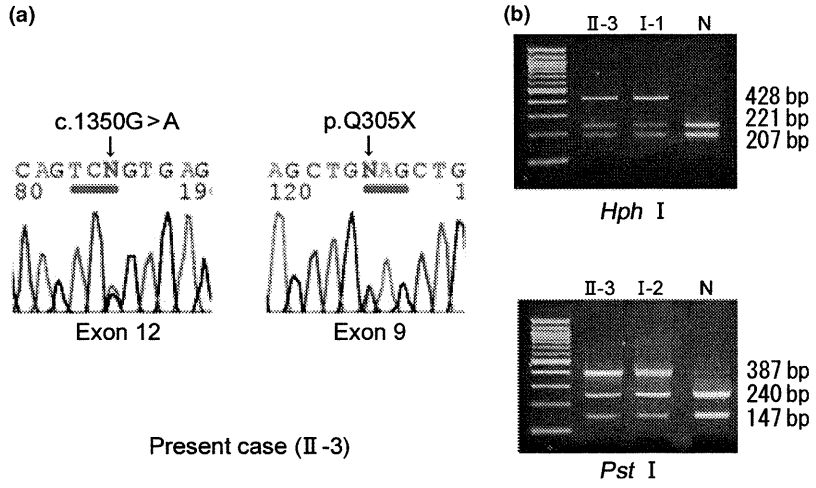

Figure 2 Analysis of the plectin gene mutations in genomic DNA from amniocytes of a fetus at risk. (a) Mutation analysis of genomic DNA from amniocytes shows both the c.1350G>A mutation in exon 12 and p.Q305X mutations in exon 9. (b) The presence of the mutations was verified by restriction enzyme digestion. The paternal mutation abolished a recognition site for the *Hph*I restriction enzyme. In the case of the normal allele, the 428-bp fragment was digested to 221 bp and 207 bp (lane N), whereas in the case of the mutant allele, a 428-bp fragment resisted digestion in the PCR product (father: lane I-1; present fetus: lane II-3). The maternal mutation also abolished a recognition site for the *Pst*I restriction enzyme. In the case of the normal allele, the 387-bp fragment was digested to 240 bp and 147 bp (lane N), whereas in the case of the mutant allele, a 387-bp fragment resisted digestion in the PCR product (mother: lane I-2; present fetus: lane II-3)

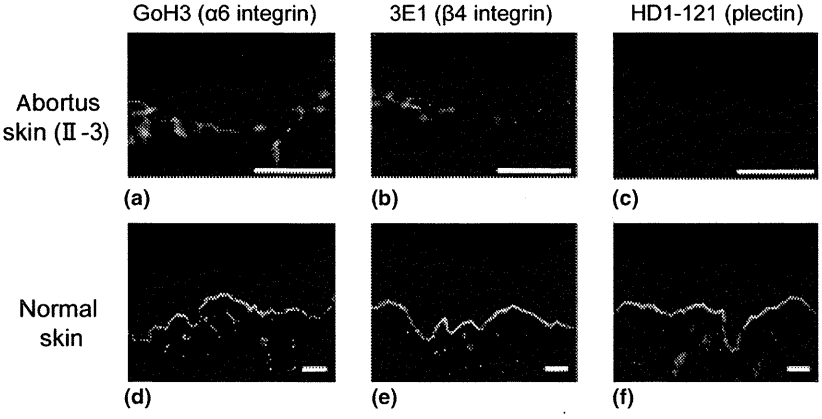

Figure 3 Absence of plectin expression in the abortus. α6 integrin (mAb GoH3) and β4 integrin (mAb 3E1) are expressed in the abortus skin (a, b) and the control skin (d, e). Staining with monoclonal antibody for plectin (mAb HD1–121) shows positive in the control skin (f) but negative in the skin of the abortus (c: blue frame). Note that the skin tissue from the abortus was subject to degeneration before skin sampling. Thus, protein localization cannot be evaluated in the degenerated tissue. Scale bar: 50 μm

was a compound-heterozygote and affected by JEB-PA. The parents elected for the fetus to be terminated at 20 weeks gestation.

Immunofluorescence analysis showed that immunoreactivity using the mAbs HD1–121 (plectin), GoH3 (α6 integrin), and 3E1 (β4 integrin) was positive in the normal control skin (Fig. 3d–f). The skin sample obtained from the abortus tested positive for α6 integrin and β4 integrin (Fig. 3a,b) but negative for plectin (Fig. 3c).

Discussion

This is the first successful PND of plectin-deficient EBS-PA, and the correct diagnosis was reconfirmed in the skin of the abortus. Given the universal mortality of EBS-PA due to *PLEC* mutations, there might be unreported PND cases for this form of EB. The prognosis of plectin-deficient EBS-PA is poor, and most patients commonly die within the first year of life,[13] as happened in the first- and

second-born progeny in the present family. Fetuses at risk of this condition are frequently terminated during pregnancy, and DNA-based PND plays an important role in prohibiting unnecessary termination of healthy fetuses at risk. Due to the recent elucidation of the causative genetic defects for genetic skin disorders, it has become possible to make DNA-based PND for severe genodermatoses by sampling of the chorionic villus or amniotic fluid in the earlier stages of pregnancy with a lower risk to fetal health and with a reduced burden on the mothers.

Plectin, a component of the hemidesmosome inner plaque, is involved in the attachment and crosslinking of the cytoskeleton and intermediate filaments to specific membrane complexes.[10] It has been described that EBS associated with muscular dystrophy (EBS-MD) results from *PLEC* mutations.[14,15] Mutations in the rod domain of *PLEC* are known to cause EBS-MD.[9,14,15] In addition, recent reports have confirmed that some *PLEC* mutations also lead to EBS-PA.[7–9,13] One alternative splice *PLEC* mRNA transcript that lacks exon 31 encoding the central core rod domain was identified in rat tissues.[16] By plectin-domain-specific reverse transcriptase-PCR, expression of this rodless alternative spliced form was confirmed in human keratinocytes.[17] Recently, our group demonstrated that loss of the full-length plectin with maintenance of the rodless plectin leads to EBS-MD, whereas complete loss or marked attenuation of full-length and rodless plectin expression underlies the EBS-PA phenotype.[12] The present family further supports the hypothesis that homozygotes or compound-heterozygotes for mutations that cause plectin truncation outside the rod domain show the EBS-PA phenotype.

In summary, this is the first report of DNA-based PND of EBS-PA. EBS-PA has now been added to the list of severe genodermatosis for which DNA-based PND is feasible.

Acknowledgments

This work was supported in part by Grants-in-Aid for Scientific Research from the Ministry of Education, Culture, Sports, Science and Technology of Japan to H. Nakamura (Kiban C 1959129107) and H. Shimizu (Kiban A 21249063).

References

1 Fine JD, Eady RA, Bauer EA, *et al.* The classification of inherited epidermolysis bullosa (EB): Report of the Third International Consensus Meeting on Diagnosis and Classification of EB. *J Am Acad Dermatol* 2008; **58**: 931–950.
2 Shimizu H. Prenatal diagnosis of epidermolysis bullosa. *Prenat Diagn* 2006; **26**: 1260–1261.
3 Pfendner EG, Nakano A, Pulkkinen L, *et al.* Prenatal diagnosis for epidermolysis bullosa: a study of 144 consecutive pregnancies at risk. *Prenat Diagn* 2003; **23**: 447–456.
4 D'Alessio M, Zambruno G, Charlesworth A, *et al.* Immunofluorescence analysis of villous trophoblasts: a tool for prenatal diagnosis of inherited epidermolysis bullosa with pyloric atresia. *J Invest Dermatol* 2008; **128**: 2815–2819.
5 Fassihi H, Renwick PJ, Black C, *et al.* Single cell PCR amplification of microsatellites flanking the COL7A1 gene and suitability for preimplantation genetic diagnosis of Hallopeau-Siemens recessive dystrophic epidermolysis bullosa. *J Dermatol Sci* 2006; **42**: 241–248.
6 Fassihi H, Liu L, Renwick PJ, *et al.* Development and successful clinical application of preimplantation genetic haplotyping for Herlitz junctional epidermolysis bullosa. *Br J Dermatol* 2010; in Press.
7 Nakamura H, Sawamura D, Goto M, *et al.* Epidermolysis bullosa simplex associated with pyloric atresia is a novel clinical subtype caused by mutations in the plectin gene (PLEC1). *J Mol Diagn* 2005; **7**: 28–35.
8 Pfendner E, Uitto J. Plectin gene mutations can cause epidermolysis bullosa with pyloric atresia. *J Invest Dermatol* 2005; **124**: 111–115.
9 Sawamura D, Goto M, Sakai K, *et al.* Possible involvement of exon 31 alternative splicing in phenotype and severity of epidermolysis bullosa caused by mutations in PLEC1. *J Invest Dermatol* 2007; **127**: 1537–1540.
10 Rezniczek GA, Walko G, Wiche G. Plectin gene defects lead to various forms of epidermolysis bullosa simplex. *Dermatol Clin* 2010; **28**: 33–41.
11 Shimizu H, Takizawa Y, Pulkkinen L, *et al.* Epidermolysis bullosa simplex associated with muscular dystrophy: phenotype-genotype correlations and review of the literature. *J Am Acad Dermatol* 1999; **41**: 950–956.
12 Natsuga K, Nishie W, Akiyama M, *et al.* Plectin expression patterns determine two distinct subtypes of epidermolysis bullosa simplex. *Hum Mutat* 2010; **31**: 308–316.
13 Pfendner E, Rouan F, Uitto J. Progress in epidermolysis bullosa: the phenotypic spectrum of plectin mutations. *Exp Dermatol* 2005; **14**: 241–249.
14 McLean WH, Pulkkinen L, Smith FJ, *et al.* Loss of plectin causes epidermolysis bullosa with muscular dystrophy: cDNA cloning and genomic organization. *Genes Dev* 1996; **10**: 1724–1735.
15 Smith FJ, Eady RA, Leigh IM, *et al.* Plectin deficiency results in muscular dystrophy with epidermolysis bullosa. *Nat Genet* 1996; **13**: 450–457.
16 Elliott CE, Becker B, Oehler S, *et al.* Plectin transcript diversity: identification and tissue distribution of variants with distinct first coding exons and rodless isoforms. *Genomics* 1997; **42**: 115–125.
17 Koster J, van Wilpe S, Kuikman I, *et al.* Role of binding of plectin to the integrin beta4 subunit in the assembly of hemidesmosomes. *Mol Biol Cell* 2004; **15**: 1211–1223.

[2] Gudbjartsson DF, Thorvaldsson T, Kong A, Gunnarsson G, Ingolfsdottir A. Allegro version 2. Nat Genet 2005;37:1015–6.
[3] Matise TC, Chen F, Chen W, De La Vega FM, Hansen M, He C, et al. A second-generation combined linkage physical map of the human genome. Genome Res 2007;17:1783–6.

Musharraf Jelani
Muhammad Tariq
Department of Biochemistry, Faculty of Biological Sciences, Quaid-i-Azam University, Islamabad, Pakistan

Iftikhar Ahmad Jan
Hazrat Ullah
Department of Pediatric Surgery, National Institute of Rehabilitation Medicine (NIRM), Islamabad, Pakistan

Muhammad Naeem
Department of Biotechnology, Faculty of Biological Sciences, Quaid-i-Azam University, Islamabad, Pakistan

Wasim Ahmad*
Department of Biochemistry, Faculty of Biological Sciences, Quaid-i-Azam University, Islamabad, Pakistan

*Corresponding author. Tel.: +92 51 90643003; fax: +92 51 9205753
E-mail address: ahmad115@hotmail.com
wahmad@qau.edu.pk (W. Ahmad)

30 June 2010
doi:10.1016/j.jdermsci.2010.11.014

Letter to the Editor

New insight into genotype/phenotype correlations in *ABCA12* mutations in harlequin ichthyosis

Harlequin ichthyosis (HI) is a severe and often fatal congenital ichthyosis with an autosomal recessive inheritance pattern [1]. The clinical features include thick, plate-like scales with ectropion, eclabium and flattened ears. *ABCA12* mutations underlie HI [2,3] and it was clarified that HI is caused by severe functional defects in the keratinocyte lipid transporter ABCA12 [2]. To date, various *ABCA12* mutations have been reported in HI patients [4]. However, genotype/phenotype correlations in *ABCA12* mutations have been poorly elucidated. In order to obtain clues to understand genotype/phenotype correlations in *ABCA12* mutations, we report two HI patients from two independent Japanese families, who were compound heterozygotes for *ABCA12* mutations.

Patient 1 is the second child of healthy, unrelated Japanese parents. The skin of the baby girl was covered with white, diamond shaped plaques at birth (Fig. 1a). After therapy with oral retinoids and local application of white petrolatum, in a humid incubator, the scales gradually detached and passive and spontaneous mobility of the joints increased. Now at the age of 1 year and 7 months, her general condition is good, although she still has white to grey scales on a background of erythematous skin over her entire body. Patient 2 is the fourth child of healthy, unrelated Japanese parents. Her older brother had a history of congenital ichthyosis and died in early infancy. The skin of the newborn showed serious symptoms with thick, white, diamond shaped plaques, partly bordered by bleeding fissures (Fig. 1c). Although she had therapy with oral retinoids and local application of white petrolatum, in a humid incubator, her clinical symptoms failed to show any apparent improvement and she died when she was 5 months old.

Skin biopsies showed thick stratum corneum in both patients (Fig. 1d–g). In Patient 2, parakeratosis was observed in the epidermis and a sparse inflammatory cell infiltration was seen in the superficial dermis (Fig. 1e inset). Electron microscopy (Hitachi, Tokyo, Japan) revealed a large number of abnormal, variously sized lipid droplets that accumulated in the cornified cells of both patients' epidermis.

Mutational analysis of *ABCA12* was performed in both patients and their families. Each genomic DNA sample was subjected to PCR amplification, followed by direct automated sequencing. Oligonucleotide primers and PCR conditions used for amplification of all exons 1–53 of *ABCA12* were originally derived from the report by Lefèvre et al. [5] and were partially modified for the present study. The entire coding region including the exon/intron boundaries for both forward and reverse strands from the patients, their parents and 50 healthy Japanese controls were also sequenced. Both patients had the same paternal novel nonsense mutation p.Arg1515X (Fig. 1h) which leads to truncation of the first ATP-binding cassette within ABCA12 likely resulting in ABCA12 loss of function (Fig. 2a). On the other allele, Patient 1 had a maternal recurrent splice acceptor site mutation c.3295-2A>G (Fig. 1h). This splice site mutation was reported in an unrelated Japanese family with HI and was shown to lead to comparable amounts of 2 splice pattern variants [2]. The first mutant transcript would result in a 3 amino acids deletion (1099_1101delYMK). These 3 amino acids are located in the first transmembrane domain and are highly conserved (Fig. 2b). The second mutant transcript lost a 170-bp sequence from exon 24, which led to a frameshift. Expression of a small amount of ABCA12 protein, although mutated, was detected in the granular layer keratinocytes of the patient's epidermis and cultured keratinocytes by immunofluorescent staining [2]. Thus, it is possible that Patient 1 expresses some mutated ABCA12 protein with a partial function. This might be the reason why Patient 1 survived beyond the perinatal and neonatal period and is still alive although this might also be in part due to the prompt oral retinoid treatment.

Patient 2 carried a maternal missense mutation p.Gly1179Arg on the other locus (Fig. 1h). To confirm the presence of the mutation p.Gly1179Arg in Patient 2, we performed restriction enzyme digestion analysis using *BclI* (NEW ENGLAND BioLabs). Restriction enzyme digestion of PCR products was carried out according to the manufacture's protocols. The 255-bp PCR products from wild type alleles were not digested by *BclI*, although the PCR products from the allele with the mutation p.Gly1179Arg were digested into 173- and 82-bp fragments. The father's PCR product after *BclI* digestion showed a single 255-bp band, which indicated he had only normal alleles. In contrast, the PCR product after *BclI* digestion from the mother of Patient 2 showed 255-, 173- and 82-bp bands, which indicated that she was heterozygous for the p.Gly1179Arg missense mutation (supplementary Fig. S1). This mutation was reported in a

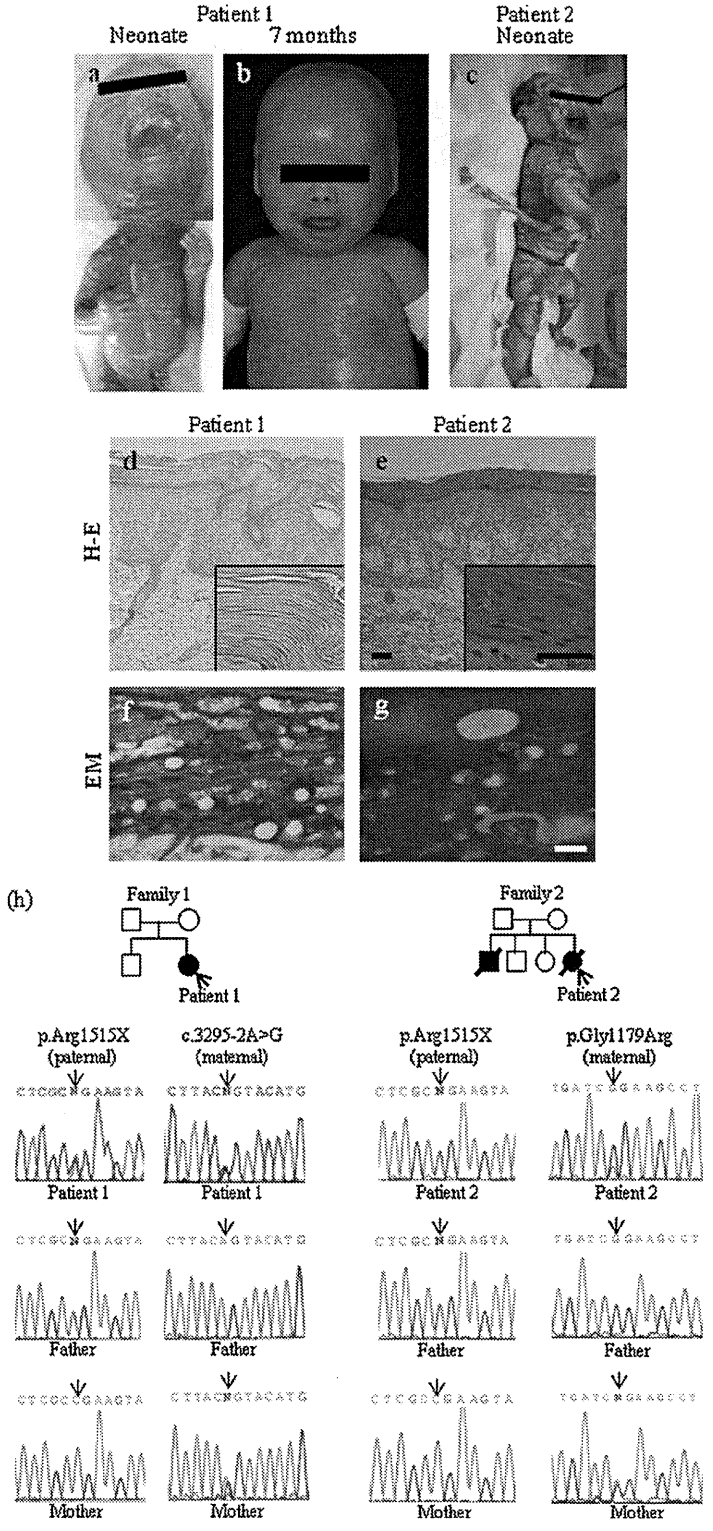

Fig. 1. (a–c) Clinical features of HI patients. Patient 1 showed the typical clinical phenotype of HI during the neonatal period, including the face and trunk (a). Her clinical symptoms remarkably improved at 7 months of age (b). Patient 2 showed more serious symptoms with thick plate-like scales and skin fissures in the neonatal period (c) and lived until the age of 5 months. (d–g) Histological features of the skin lesions of HI patients. Skin biopsies showed thick stratum corneum in both patients. Bars, 50 μm (d and e). In Patient 2, parakeratosis were observed (e, inset). By electron microscopy, abnormal variously sized lipid droplets had accumulated in the cornified cells of both patients' epidermis. Bars, 200 nm (f and g). (h) Families with HI and *ABCA12* mutations. Patient 1 was a compound heterozygote for two *ABCA12* mutations, a novel nonsense mutation p.Arg1515X and a recurrent splice site mutation c.3295-2A>G, and both her parents were heterozygous carriers. Patient 2 harboured two *ABCA12* mutations, p.Arg1515X and p.Gly1179Arg, and both her parents were heterozygous carriers of these defects.

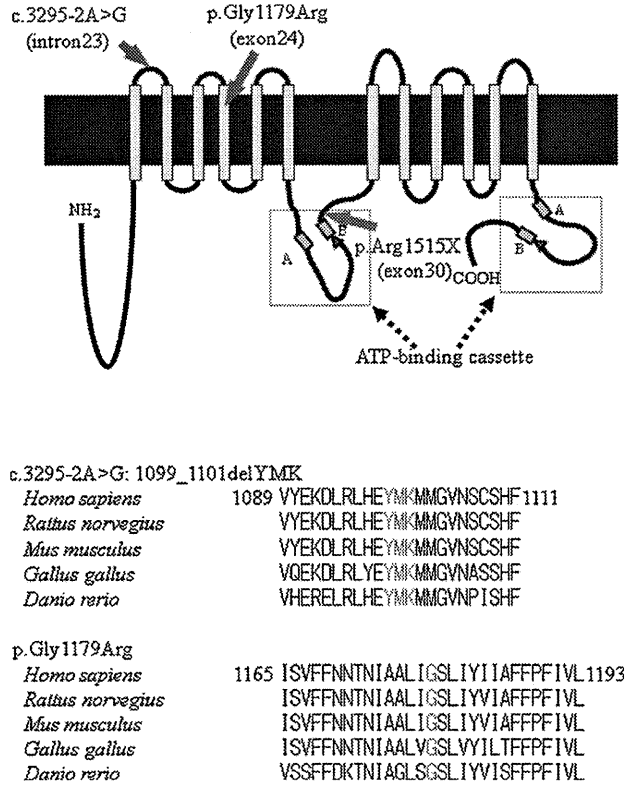

Fig. 2. (a) Structure of ABCA12 protein and the three mutations in present HI families. Dark blue area, cell membrane; bottom of dark-blue area, cytoplasmic surface. Note the mutation shared between the two patients is a truncation mutation in the first ATP-binding cassette (p.Arg1515X). The other mutation in Patient 2 is just a missense mutation in the first cluster of transmembrane domains (p.Gly1179Arg). (b) ABCA12 amino acid sequence alignment shows the level of conservation in diverse species of the amino acids, 1099_1101delYMK and p.Gly1179Arg (red characters).

Laotian family [6]. The glycine 1179 is a highly conserved amino acid residue (Fig. 2b) located in the first transmembrane ABCA12 domain (Fig. 2a), and this mutation substitutes an uncharged polar glycine residue for a positively charged arginine residue. The presence of these mutations was excluded in 100 alleles of 50 normal unrelated Japanese individuals.

Determinants of genotype/phenotype correlations resulting from *ABCA12* mutations, typically demonstrate that homozygotes or compound heterozygotes with truncation *ABCA12* mutations lead to an HI phenotype. Only a few exceptional cases have been reported such as the present case. The mutation p.Gly1179Arg might result in major loss of ABCA12 function and/or structure, leading to the severe phenotype in Patient 2.

Recently, long-term survival of patients with HI has been more frequently observed and documented [7,8]. The clinical symptoms of Patient 1 showed a remarkable improvement during infancy. In contrast, the symptoms of Patient 2 did not improve, and she died at the age of 5 months. The marked difference in the clinical severity of the two patients indicated that the p.Gly1179Arg has far bigger deleterious functional effects than c.3295-2A>G. The present study clearly demonstrates that some missense *ABCA12* mutations within highly conserved transmembrane regions are able to cause drastic changes in protein structure and function, leading to severe phenotypes, similar to truncation mutation patients. Further accumulation of similar cases is needed to confirm genotype/phenotype correlation in *ABCA12* mutations, especially in studies involving missense mutations underlying HI.

Acknowledgments

We thank Dr. James R. McMillan for proofreading the manuscript. This work was supported in part by a grant-in-aid from the Ministry of Education, Science, Sports and Culture of Japan (Kiban B 20390304: to M.A.), a grant from Ministry of Health, Labour and Welfare of Japan (Health and Labour Sciences Research Grants; Research on Intractable Disease: H22-177: to M.A.).

Appendix A. Supplementary data

Supplementary data associated with this article can be found, in the online version, at doi:10.1016/j.jdermsci.2010.11.010.

References

[1] Akiyama M. Harlequin ichthyosis and other autosomal recessive congenital ichthyoses: the underlying genetic defects and pathomechanisms. J Dermatol Sci 2006;42:83–9.
[2] Akiyama M, Sugiyama-Nakagiri Y, Sakai K, McMillan JR, Goto M, Arita K, et al. Mutations in ABCA12 in harlequin ichthyosis and functional rescue by corrective gene transfer. J Clin Invest 2005;115:1777–84.
[3] Kelsell DP, Norgett EE, Unsworth H, Teh MT, Cullup T, Mein CA, et al. Mutations in ABCA12 underlie the severe congenital skin disease harlequin ichthyosis. Am J Hum Genet 2005;76:794–803.
[4] Akiyama M. ABCA12 mutations and autosomal recessive congenital ichthyosis: a review of genotype/phenotype correlations and of pathogenetic concepts. Hum Mutat 2010;31(July):1090–6.
[5] Lefèvre C, Audebert S, Jobard F, Bouadjar B, Lakhdar H, Boughdene-Stambouli O, et al. Mutations in the transporter ABCA12 are associated with lamellar ichthyosis type 2. Hum Mol Genet 2003;12:2369–78.
[6] Thomes AC, Cullup T, Norgett EE, Hill T, Barton S, Dale BA, et al. ABCA12 is the major harlequin ichthyosis gene. J Invest Dermatol 2006;126:2408–13.
[7] Akiyama M, Sakai K, Sato T, McMillan JR, Goto M, Sawamura D, et al. Compound heterozygous ABCA12 mutations including a novel nonsense mutation underlie harlequin ichthyosis. Dermatology 2007;215:155–9.
[8] Akiyama M, Sakai K, Wolff G, Hausser I, McMillan JR, Sawamura D, et al. A novel ABCA12 mutation 327delT causes harlequin ichthyosis. Br J Dermatol 2006;155:1064–6.

H. Umemoto[a,b]
[a]*Department of Dermatology, Hokkaido University Graduate School of Medicine, Sapporo, Japan*
[b]*Department of Oral Diagnosis and Oral Medicine, Hokkaido University Graduate School of Dental Medicine, Sapporo, Japan*

M. Akiyama[a,b,*]
[a]*Department of Dermatology, Hokkaido University Graduate School of Medicine, Sapporo, Japan*
[b]*Department of Dermatology, Nagoya University Graduate School of Medicine, Nagoya, Japan*

T. Yanagi
K. Sakai
Department of Dermatology, Hokkaido University Graduate School of Medicine, Sapporo, Japan

Y. Aoyama
Department of Dermatology, Okayama University Graduate School of Medicine, Okayama, Japan

A. Oizumi
Y. Suga
Department of Dermatology, Juntendo University School of Medicine, Urayasu Hospital, Urayasu, Japan

DOI:10.1111/j.1600-0625.2010.01177.x
www.blackwellpublishing.com/EXD

Letter to the Editor

A founder effect of c.1938delC in *ITGB4* underlies junctional epidermolysis bullosa and its application for prenatal testing

Ken Natsuga[1], Wataru Nishie[1], Satoru Shinkuma[1], Hideki Nakamura[1], Ken Arita[1], Kozo Yoneda[2], Takashi Kusaka[3], Toshihiro Yanagihara[4], Rika Kosaki[5], Haruhiko Sago[6], Masashi Akiyama[1] and Hiroshi Shimizu[1]

[1]Department of Dermatology, Hokkaido University Graduate School of Medicine, Sapporo, Japan;
[2]Department of Dermatology, Kagawa University, Kagawa, Japan;
[3]Department of Pediatrics, Kagawa University, Kagawa, Japan;
[4]Department of Perinatology and Gynecology, Kagawa University, Kagawa, Japan;
[5]Division of Clinical Genetics and Molecular Medicine, National Center for Child Health and Development, Tokyo, Japan;
[6]Department of Maternal-Fetal and Neonatal Medicine, National Center for Child Health and Development, Tokyo, Japan
Correspondence: Ken Natsuga, MD, PhD, Department of Dermatology, Hokkaido University Graduate School of Medicine, North 15 West 7, Sapporo 060-8638, Japan, Tel.: +81 11 716 1161, ext. 5962, Fax: +81 11 706 7820, e-mail: natsuga@med.hokudai.ac.jp

Abstract: Junctional epidermolysis bullosa associated with pyloric atresia (JEB-PA) is one of the most severe inherited skin diseases, characterized by generalized blister formation and occlusion of the pylorus at birth. Most JEB-PA patients have mutations in the gene encoding β4 integrin (*ITGB4*). No recurrent mutations in *ITGB4* have been described as having founder effects. We collected three JEB-PA families with c.1938delC in *ITGB4*. Haplotype analysis using single nucleotide polymorphism markers throughout *ITGB4* suggested one rare haplotype (2.8% of the Han Chinese and ethnic Japanese populations) in all alleles with c.1938delC. The parents of one of the three families sought prenatal diagnosis for a subsequent pregnancy. We succeeded in performing prenatal exclusion of JEB-PA using the foetal genomic DNA. Our study clearly demonstrated that recurrent c.1938delC in *ITGB4* is a founder mutation in JEB-PA patients, and that genotyping of the mutation can be utilized for prenatal diagnosis of JEB-PA.

Key words: basement membrane zone – haplotype analysis – single nucleotide polymorphism

Accepted for publication 20 July 2010

Background

Recurrent mutations in a population might be explained by founder effects, in which the mutant alleles of a few ancestors spread in the population because of limited gene pool, genetic drift and healthy carrier migration (1).

Epidermolysis bullosa (EB) comprises a group of disorders characterized by congenital skin fragility. EB has been classified into EB simplex, junctional epidermolysis bullosa (JEB), dystrophic EB and Kindler syndrome (2–4). JEB is subclassified into three clinical subtypes: Herlitz JEB, non-Herlitz JEB and JEB with pyloric atresia (JEB-PA). JEB-PA is characterized by generalized blistering and occlusion of the pylorus at birth, which usually leads to early demise (5). Mutations in the gene encoding α6 (*ITGA6*) or the β4 integrin subunit (*ITGB4*) are responsible for JEB-PA (6,7). Most patients with JEB-PA have mutations in *ITGB4* (8). No frequent prevalent mutations have been noted, except in the Hispanic population, where c.1802G>A (p.Cys601Tyr) is present on five of 10 alleles of JEB-PA patients (9).

Here, we have collected three JEB-PA families, in which c.1938delC in *ITGB4* is present. Haplotype analysis revealed c.1938delC as a founder mutation in JEB patients. Based on these data, we successfully performed prenatal exclusion of JEB-PA with this mutation.

Experimental design

Patients

Three unrelated non-consanguineous Japanese families (A, B and C) with JEB-PA in this study are summarized in Fig. S1a. Family A and B originate from Shikoku Island in Japan and family C is from other part of the country. A-1 and B-1 are newly identified JEB-PA patients. They died of disseminated intravascular coagulation 1 and 2 months after birth, respectively. Immunofluorescence study of skin specimens from both of the patients showed the absence of β4 integrin and weak expression of α6 integrin subunits (data not shown). Immunostaining for laminin 332, type IV collagen, type VII collagen, type XVII collagen, plectin and BP230 revealed normal linear labelling patterns (data not shown). C-2 is a patient with non-lethal variant of JEB-PA. The case description and mutational data of C-2 have been reported previously (10).

Mutation detection

Genomic DNA (gDNA) was extracted from blood cells of the probands and their parents. Mutation detection was performed after polymerase chain reaction (PCR) amplification of all exons and intron–exon borders of *ITGB4*, followed by direct sequencing using an ABI Prism 3100 genetic analyzer (Advanced Biotechnologies Inc., Columbia, MD, USA) (11–13). The genomic DNA nucleotides, the complementary DNA nucleotides and the amino

acids of the protein were numbered based on the following sequence information (GenBank accession No. NM_000213).

Haplotype analysis

To determine whether c.1938delC is a founder mutation, we performed haplotype analysis of three JEB-PA families. We constructed linkage disequilibrium (LD) blocks containing *ITGB4* using genotype data from the HapMap database (International HapMap Consortium, 2005). The haplotype structure with its tag-single nucleotide polymorphisms (SNPs) was determined using Haploview (14). We genotyped 15 tag-SNPs (Fig. S1b) using the ABI Prism 3100 genetic analyzer (Advanced Biotechnologies Inc.).

Prenatal diagnosis

We performed prenatal diagnosis of a foetus (A-2) at risk for JEB-PA from family A. A total of 30 ml of amniotic fluid was obtained under ultrasound guidance at 16 weeks' gestation. Foetal DNA was extracted from fresh cells from 10 ml of amniotic fluid. Genomic DNA isolated from amniotic fluid cells was subjected to polymerase chain reaction (PCR) amplification, followed by direct automated sequencing as described. The mutation site was sequenced using both forward and reverse strands and verified by *PmlI* (New England Biolabs Inc., Beverly, MA, USA) enzyme digestion of the PCR products.

The medical ethical committee of Hokkaido University and National Center for Child Health and Development approved all described studies. The study was conducted according to Declaration of Helsinki Principles. Participants gave their written informed consent.

Results

Recurrent c.1938delC in *ITGB4*

ITGB4 mutation analysis revealed that A-1 was homozygous for c.1938delC (Fig. 1c). The father and mother of A-1 were heterozygous for c.1938delC (Fig. 1a, b). B-1 was heterozygous for paternal c.1938delC and maternal c.4050_4057del (data not shown). c.1938delC was previously described in a patient with non-lethal variant of JEB-PA who is compound heterozygous for c.1938delC and c.2168C>G (p.Pro723Arg) (C-2) (10). c.4050_4057del was also reported in a JEB-PA patient who is compound heterozygous for c.4050_4057del and c.3434delT (12).

Founder effects of c.1938delC

The haplotype structure containing *ITGB4* was constructed using genotype data from the HapMap database (Fig. S1b, c). The haplotype block was represented by 16 haplotypes with >2% frequency (Fig. S1b, c). The chromosome containing c.1938delC in A-1 and B-1 had haplotype XI (GGGACGGGCGTCACC), which is seen in 2.8% of the Han Chinese and ethnic Japanese populations. The chromosome containing c.1938delC in C-2 might have had this haplotype although the phase was not determined.

Prenatal exclusion of JEB-PA

Direct sequencing of PCR products from the foetal gDNA (A-2) revealed the presence of c.1938delC in one allele and wild-type sequence in another allele (Fig. 1d). To confirm the results of direct sequencing, we performed restriction enzyme analysis. c.1938delC was found to result in the loss of a restriction enzyme for *PmlI*. The PCR product from the proband (A-1) after *PmlI* digestion revealed a 285-bp band, which indicated that she was homozygous for c.1938delC (Fig. 1f). In contrast, the PCR product from the parents and the foetus (A-2) after *PmlI* digestion showed 285-, 195- and 90-bp bands, which indicated that they were heterozygous for c.1938delC (Fig. 1f). Haplotype analysis of this family using microsatellite markers excluded maternal contamination of foetal cells (data not shown). These results predicted that the foetus would not be affected, and the pregnancy was continued. A neonate was born at full term in good health with completely normal skin.

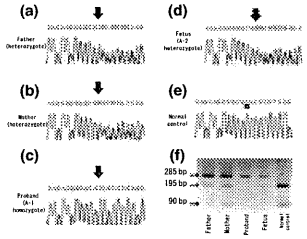

Figure 1. Prenatal diagnosis of junctional epidermolysis bullosa with pyloric atresia (family A). (a–e) Direct sequencing of *ITGB4*. The parents were heterozygous for c.1938delC in *ITGB4* (a, b). A-1, the proband, was homozygous for that mutation (c). A-2, the foetus, was found to be a heterozygous carrier (d). A cytosine at cDNA position 1938 in normal control is underlined (e). Arrows indicate a deleted cytosine in *ITGB4* sequence. (f) *PmlI* restriction enzyme digestion of the PCR products from the family members' genomic DNA. c.1938delC results in the loss of a site for *PmlI*. *PmlI* restriction enzyme digestion of the PCR products from normal control reveals 195- and 90-bp bands. Only a 285-bp band is observed in A-1 (the proband), who is homozygous for c.1938delC. In contrast, 285-, 195- and 90-bp bands are detected in the father, mother and A-2, suggesting that they are heterozygous for c.1938delC.

Conclusions

There are no recurrent *ITGB4* mutations that have been demonstrated to have founder effects in JEB-PA patients. Our study detected recurrent c.1938delC in *ITGB4* and revealed this to be a founder mutation in JEB-PA patients.

DNA-based prenatal testing of JEB-PA has been described (15–18). Our study has demonstrated the successful prenatal exclusion of JEB-PA with c.1938delC through mutation analysis of the foetal genomic DNA.

In summary, our study identified a founder c.1938delC in *ITGB4* and showed that this mutation can be applied for prenatal diagnosis of JEB-PA.

Acknowledgements

We thank Ms Yuko Hayakawa and Ms Yuki Miyamura for their technical assistance. This work was supported by Health and Labor Sciences Research grants for Research on Measures for Intractable Diseases from the Ministry of Health, Labor and Welfare of Japan (to H.S.).

Conflicts of interest

The authors declare no conflicts of interest.

References

1 Castiglia D, Zambruno G. Dermatol Clin 2010: **28**: 17–22.
2 Bowden P E, Knight A G, Liovic M. Exp Dermatol 2009: **18**: 650–652.
3 Dang N, Murrell D F. Exp Dermatol 2008: **17**: 553–568.
4 Fine J D, Eady R A, Bauer E A *et al.* J Am Acad Dermatol 2008: **58**: 931–950.
5 Chung H J, Uitto J. Dermatol Clin 2010: **28**: 43–54.
6 Ruzzi L, Gagnoux-Palacios L, Pinola M *et al.* J Clin Invest 1997: **99**: 2826–2831.

7 Vidal F, Aberdam D, Miquel C *et al.* Nat Genet 1995: **10**: 229–234.
8 Dang N, Klingberg S, Rubin A I *et al.* Acta Derm Venereol 2008: **88**: 438–448.
9 Varki R, Sadowski S, Pfendner E *et al.* J Med Genet 2006: **43**: 641–652.
10 Abe M, Sawamura D, Goto M *et al.* J Dermatol Sci 2007: **47**: 165–167.
11 Natsuga K, Nishie W, Arita K *et al.* J Invest Dermatol 2010: **130**: 2671–2674.
12 Takizawa Y, Shimizu H, Nishikawa T *et al.* J Invest Dermatol 1997: **108**: 943–946.
13 Nakano A, Pulkkinen L, Murrell D *et al.* Pediatr Res 2001: **49**: 618–626.
14 Barrett J C, Fry B, Maller J *et al.* Bioinformatics 2005: **21**: 263–265.
15 Shimizu H. Prenat Diagn 2006: **26**: 1260–1261.
16 Ashton G H, Sorelli P, Mellerio J E *et al.* Br J Dermatol 2001: **144**: 408–414.
17 Gache Y, Romero-Graillet C, Spadafora A *et al.* J Invest Dermatol 1998: **111**: 914–916.
18 Pfendner E G, Nakano A, Pulkkinen L *et al.* Prenat Diagn 2003: **23**: 447–456.

Supporting Information

Additional Supporting Information may be found in the online version of this article:

Figure S1. Haplotype analysis of the junctional epidermolysis bullosa families.

Please note: Wiley-Blackwell are not responsible for the content or functionality of any supporting materials supplied by the authors. Any queries (other than missing material) should be directed to the corresponding author for the article.

DOI:10.1111/j.1600-0625.2010.01172.x
www.blackwellpublishing.com/EXD

Letter to the Editor

IL-1 signalling is dispensable for protective immunity in *Leishmania*-resistant mice

Kordula Kautz-Neu[1]*, Susanna L. Kostka[1]*, Stephanie Dinges[1], Yoichiro Iwakura[2,3], Mark C. Udey[4] and Esther von Stebut[1]

[1]Department of Dermatology, Johannes-Gutenberg University, Mainz, Germany;
[2]Center for Experimental Medicine and Systems Biology, Institute of Medical Science, University of Tokyo, Tokyo, Japan;
[3]Core Research for Evolutional Science and Technology (CREST), Japan Science and Technology Agnecy, Saitama, Japan;
[4]Dermatology Branch, NCI, NIH, Bethesda, MD, USA
Correspondence: Esther von Stebut, Department of Dermatology, Johannes-Gutenberg University, Langenbeckstrasse 1, 55131 Mainz, Germany, Tel.: +49-6131-175731, Fax: +49-6131-173470, e-mail: vonstebu@uni-mainz.de
*Both authors contributed equally.

Abstract: Leishmaniasis is a parasitic disease affecting ~12 million people. Control of infection (e.g. in C57BL/6 mice) results from IL-12-dependent production of IFNγ by Th1/Tc1 cells. In contrast, BALB/c mice succumb to infection because of preferential Th2-type cytokine induction. Infected dendritic cells (DC) represent important sources of IL-12. Genetically determined differences in DC IL-1α/β production contribute to disease outcome. Whereas the course of disease was not dramatically altered in IL-1RI$^{-/-}$ mice, local administration of IL-1α to infected C57BL/6 mice improved disease outcome. To definitively elucidate the involvement of IL-1 in immunity against leishmaniasis, we now utilized IL-1α/β-double-deficient C57BL/6 mice. C57BL/6 mice are believed to be a good surrogate model for human, self limited cutaneous leishmaniasis (CL). *Leishmania major*-infected IL-1α/β$^{-/-}$ mice were resistant to experimental CL comparable to controls. In addition, DC-based vaccination against leishmaniasis in C57BL/6 mice was independent of IL-1. Thus, in *Leishmania*-resistant C57BL/6 mice, IL-1 signalling is dispensable for protection.

Key words: IL-1 – dendritic cells – *L. major*

Accepted for publication 26 July 2010

Background

Leishmaniasis is a parasitic disease transmitted by the bite of a sand fly. The disease ranges from cutaneous leishmaniasis (CL) to visceral leishmaniasis and ~12 million people are affected worldwide (1). In murine experimental leishmaniasis, control of infection results from IL-12-dependent production of Th1/Tc1-derived IFNγ that activates infected macrophages (MΦ) to eliminate parasites (2–5). In disease-resistant C57BL/6 mice, skin DC infected with *Leishmania major* represent important sources of IL-12 (6). In contrast, BALB/c mice respond to infection with preferential Th2-type cytokine production, which is associated with disease progression.

Abbreviations: CL, cutaneous leishmaniasis; DC, dendritic cells; MΦ, macrophages.

Genetically determined DC-derived factors that influence disease susceptibility of BALB/c mice include elevated levels of inhibitory IL-12p80 (7) and decreased release of IL-1α/β (8,9). Previously, we demonstrated that IL-1α/β facilitates Th1 induction in several inflammatory disease models (9–11). Treatment of BALB/c mice with IL-1 during T cell priming inhibited progressive disease by shifting the immune response towards Th1 (9). However, prolonged administration of IL-1α promoted Th2 expansion in already established infections and worsened disease outcome (11).

Question addressed

IL-1 is a key mediator of inflammation (12,13). IL-1α and IL-1β exert similar biological functions by binding to the IL-1 type I receptor (IL-1RI) (14). To definitively elucidate the involvement of IL-1 in immune responses in CL, we utilized IL-1α/β-double

thickness of the mucous layer of small intestines, resulting in the inhibition of small intestinal absorption.[4] In addition, PGE1 increases blood flow in the stomach and upregulates the digestion in the stomach. During the provocation test in our case, serum gliadin levels were not increased by administering misoprostol. However, sodium cromoglicate, a mast cell stabilizer commonly used to treat allergic rhinitis, allergic conjunctivitis, and asthma, could not affect serum gliadin levels in the provocation test, and therefore allowed the symptoms to occur. We consider that the effects of misoprostol on the alimentary tract are crucial for the prevention of FDEIA. Our observation indicates that the exacerbating effect of aspirin in FDEIA comes from the inhibitory effects of aspirin on PGE1 in the gastrointestinal milieu. Thus, misoprostol would be a promising prophylactic drug for FDEIA.

Aya Takahashi, MD
Kimiko Nakajima, MD
Mitsunori Ikeda, MD
Shigetoshi Sano, MD
Department of Dermatology
Kochi Medical School, Nankoku
Kochi
Japan

Kunie Kohno, MD
Eishin Morita, MD
Department of Dermatology
Shimane University Faculty of Medicine
Izumo, Shimane
Japan
E-mail: jm-aya.derm@kochi-u.ac.jp

References

1 Matsuo H, Morita E, Tatham AS, *et al.* Identification of the IgE-binding epitope in omega-5 gliadin, a major allergen in wheat-dependent exercise-induced anaphylaxis. *J Biol Chem* 2004; 279: 12135–40.
2 Matsuo H, Morimoto K, Akaki T, *et al.* Exercise and aspirin increase levels of circulating gliadin peptides in patients with wheat-dependent exercise-induced anaphylaxis. *Clin Exp Allergy* 2005; 35: 461–6.
3 Sheffer AL, Tong AK, Murphy GF, *et al.* Exercise-induced anaphylaxis: a serious form of physical allergy associated with mast cell degranulation. *J Allergy Clin Immunol* 1985; 75: 479–84.
4 Gurleyik E, Coskun O, Ustundag N, *et al.* Prostaglandin E1 maintains structural integrity of intestinal mucosa and prevents bacterial translocation during experimental obstructive jaundice. *J Invest Surg* 2006; 19: 283–9.

Type XVII collagen ELISA indices significantly decreased after bullous pemphigoid remission

The major pathogenic epitope of bullous pemphigoid (BP) is known to be the noncollagenous extracellular domain (NC16A) of type XVII collagen (COL17).[1] Here we investigated indirect immunofluorescence (IIF) and COL17 NC16A domain enzyme-linked immunosorbent assay (ELISA)[2–5] data before treatment and after remission to evaluate the usefulness of ELISA analyses as indicators for BP disease activity.

We included ten consecutive BP patients [eight women and two men: between 33 and 80 years old (mean; 59 years old)] who showed typical clinical features before treatment and were successfully treated, resulting in complete or partial remission at our institute. The first day of each patient visit was within the last three years. In all patients, the diagnosis was confirmed by histopathological observation and immunofluorescence study, i.e. histopathological subepidermal blister formation was observed and direct and IIF studies revealed the presence of autoantibodies along the dermal–epidermal junction. All patients were successfully treated with oral prednisolone therapy of 30–50 mg/d with or without azathioprine or a combination therapy using tetracycline and nicotinamide. Treatment periods from initial diagnosis to remission ranged from four months to 35 months (mean; 14.6 ± 10.8 months). Serum samples were obtained for ELISA and IIF at least twice during the disease course for each patient.

Concentration of autoantibodies in the patients' sera directed against the NC16A domain of COL17 was measured using the COL17 NC16A ELISA kit following the kit's instructions.[6] IIF staining and evaluation were performed as previously described using normal human skin as a substrate.[7]

In all the cases, the ELISA indices showed a decrease during the successful treatment course. ELISA indices after remission were significantly reduced compared with those before treatment ($P < 0.0001$) (Fig. 1a). IIF titers also decreased after remission in six cases, but the titers were not apparently reduced in the other four cases, although a statistically significant reduction in combined IIF titer was observed after remission compared with those before treatment ($P < 0.05$) (Fig. 1b).

Positive correlation between ELISA indices and BP disease activity has been reported previously in the literature. Di Zenzo *et al.*[8] demonstrated that disease severity before treatment was well correlated with ELISA indices in BP patients. Izumi *et al.*[9] described ELISA indices and alteration of disease activity of five BP patients during various treatments. In this study, we compared the ELISA

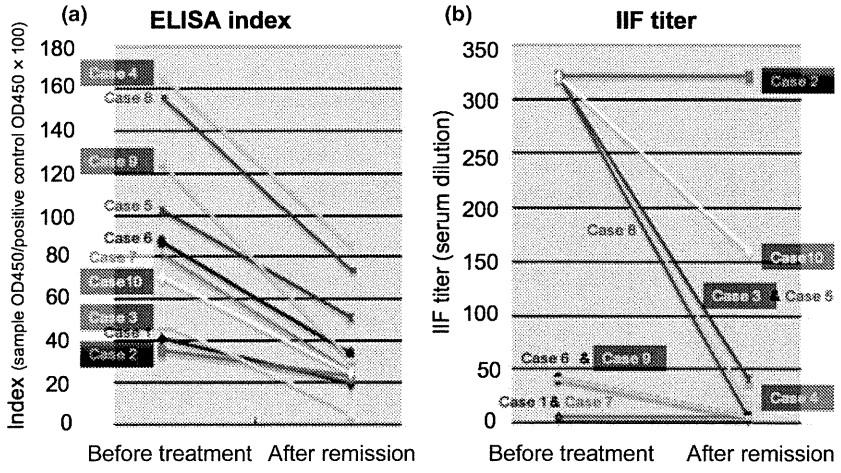

Figure 1 ELISA indices and indirect immunofluorescence (IIF) titers before treatment and after remission. (a) ELISA indices of successfully treated BP patients. Disease remission was defined as when erythema, bullae and erosions had completely healed (complete remission) or no more than three bullae or erythema were seen in a week (partial remission) and only a low dose of oral prednisolone (<5 mg/d) or no treatment was needed to maintain this condition. As ELISA indices after remission, we adopted ELISA indices at the time when each patient's disease activity was evaluated as being in "complete remission" or "partial remission" (as defined above) for the first time after treatment. Mean ELISA index of the 10 patients before treatment was 91.3 ± 45.7 (range: 35.6–165.6) and the mean index after remission was 37.4 ± 25.3 (range: 6.0–86.4). After complete or partial remission, the ELISA indices were significantly reduced ($P < 0.0001$). (b) IIF titers of the same patients. Apparent decreases in IIF titers after remission were seen only in six patients. Mean IIF titer of the 10 patients before treatment was 201 ± 154 (range: 5–320) and the mean titer after remission was 60.5 ± 102.8 (range: 5–320). A statistically, significant reduction was observed in combined IIF titers after remission compared with those before treatment ($P < 0.05$). Colors of the lines are specific for each patient in both figures (a) and (b)

indices before treatment and after remission in our BP patient cohort and clearly demonstrated that ELISA indices significantly decreased after remission. Feng *et al.*[10] reported similar results on correlation of ELISA indices with disease course in BP patients, although the time points for ELISA after treatment were just before the decrease in corticosteroid and when the dosage of corticosteroid was successfully decreased to half the initial dose in the report. In this study, we employed ELISA indices at the time when each patient's disease activity was evaluated as "complete remission" or "partial remission" for the first time after treatment. Thus, this study is unique in the point that we evaluated exact correlation between ELISA indices and disease remission.

In conclusion, the present results further support the idea that the COL17 NC16A ELISA indices demonstrate a correlation with the BP disease remission more accurately than IIF titers and are a useful tool to detect BP disease remission and to assess the efficacy of BP treatment.

Erika Kusajima
Masashi Akiyama, MD, PhD
Megumi Sato
Ken Natsuga, MD
Hiroshi Shimizu, MD, PhD
Department of Dermatology
Hokkaido University Graduate School of Medicine
Sapporo
Japan
E-mail: akiyama@med.hokudai.ac.jp
Conflict of interest: the authors state no conflict of interest.

References

1 Giudice GJ, Emery DJ, Zelickson BD, *et al.* Bullous pemphigoid and herpes gestationis autoantibodies recognize a common non-collagenous site on the BP180 ectodomain. *J Immunol* 1993; 151: 5742–5750.
2 Zillikens D, Mascaro JM, Rose PA, *et al.* A highly sensitive enzyme-linked immunosorbent assay for the detection of circulating anti-BP180 autoantibodies in patients with bullous pemphigoid. *J Invest Dermatol* 1997; 109: 679–683.
3 Hata Y, Fujii Y, Tsunoda K, Amagai M. Production of the entire extracellular domain of BP180 (type XVII collagen) by baculovirus expression. *J Dermatol Sci* 2000; 23: 183–190.
4 Schmidt E, Obe K, Brocher EB, Zillikens D. Serum levels of autoantibodies to BP180 correlate with disease activity in patients with bullous pemphigoid. *Arch Dermatol* 2000; 136: 174–178.

5 Kobayashi M, Amagai M, Kuroda-Kinoshita K, *et al.* BP180 ELISA using bacterial recombinant NC16a protein as a diagnostic and monitoring tool for bullous pemphigoid. *J Deramtol Sci* 2002; 30: 224–232.
6 Tsuji-Abe Y, Akiyama M, Yamanaka Y, *et al.* Correlation of clinical severity and ELISA indices for the NC16A domain of BP180 measured using BP180 ELISA kit in bullous pemphigoid. *J Dermatol Sci* 2005; 37: 145–149.
7 Beutner EH, Jordon RE, Chorzelski TP. The immunopathology of pemphigus and bullous pemphigoid. *J Invest Dermatol* 1968; 51: 63–80.
8 Di Zenzo G, Thoma-Uszynski S, Fontao L, *et al.* Multicenter prospective study of the humoral autoimmune response in bullous pemphigoid. *Clin Immunol* 2008; 128: 415–426.
9 Izumi T, Ichiki Y, Esaki C, Kitajima Y. Monitoring of ELISA for anti-BP180 antibodies: clinical and therapeutic analysis of steroid-treated patients with bullous pemphigoid. *J Dermatol* 2004; 31: 383–391.
10 Feng S, Wu Q, Jin P, *et al.* Serum levels of autoantibodies to BP180 correlate with disease activity in patients with bullous pemphigoid. *Int J Dermatol* 2008; 47: 225–228.

Case letters

Extremely severe palmoplantar hyperkeratosis in a generalized epidermolytic hyperkeratosis patient with a keratin 1 gene mutation

To the Editor: Epidermolytic hyperkeratosis (EHK; OMIM#113800), also called bullous congenital ichthyosiform erythroderma, is a rare genetic disorder of keratinization. We report a patient with generalized EHK showing extremely severe palmoplantar hyperkeratosis with digital contractures.

A 45-year-old Japanese man had erythroderma at birth. He exhibited skin blistering, erosions, and hyperkeratosis on the erythrodermic skin since infancy. The blistering and erosions gradually diminished with age. He developed severe palmoplantar hyperkeratosis and digital contractures at 7 years of age. At 24 years of age, surgery was performed to improve the contraction of his toes. A physical examination revealed hyperkeratosis of the entire body, especially at the ankles, elbows, and knees, and erosions were observed on the inner side of the elbows and knees (Fig 1, *A-D*). Palmoplantar hyperkeratosis was severe with digital contractures. The morphology of his hair, nails, and teeth was normal. There was no known family history of skin disease. Skin biopsy from the upper portion of the left arm showed severe granular degeneration in all the suprabasal layers (Fig 1, *E*). Ultrastructural analysis revealed clumping of the intermediate filaments within keratinocytes of the suprabasal layers (Fig 1, *F*).

Direct sequencing of the whole coding regions of *KRT1* and *KRT10* (GenBank accession numbers NT029419.11 and NT010755.15) was performed as previously described,[1] and a novel heterozygous *KRT1* missense mutation c.1457T>G (p.Leu486Arg) was identified in exon 7. This mutation was verified by restriction enzyme *Msp*I digestion. The mutation p.Leu486Arg was not found in 100 normal, unrelated Japanese alleles (50 healthy unrelated individuals) using sequence analysis (data not shown).

The present novel *KRT1* mutation p.Leu486Arg is in the 2B segment of keratin 1 (Fig 2, *A* and *B*). This mutation occurred within the highly conserved helix termination motif (HTM) of the K1 protein. The palmoplantar hyperkeratosis was extremely severe. It is noteworthy that another mutation at the identical

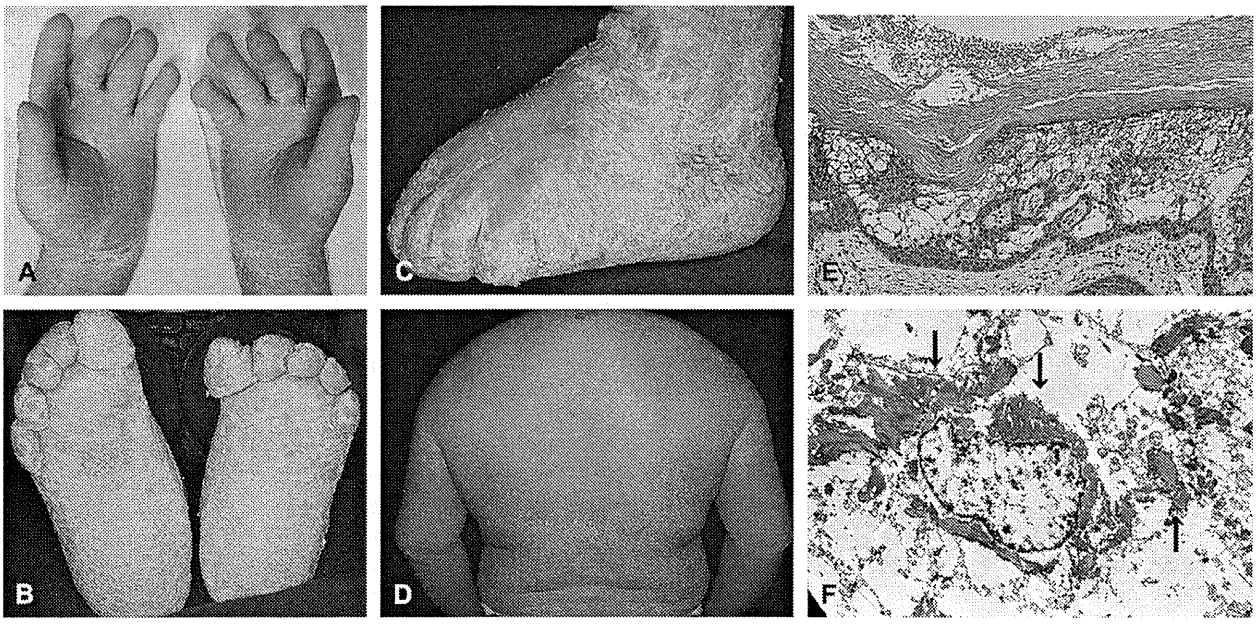

Fig 1. Clinical, histopathologic, and ultrastructural features of the patient. Severe diffuse hyperkeratosis and scale are seen on the palms (**A**) and soles (**B**). Warty brown hyperkeratosis and scale are present on the margins and the dorsal surface of the foot (**C**). Generalized erythroderma and scaling is seen on the trunk (**D**). The histopathologic examination revealed acanthosis and hyperkeratosis, coarse keratohyaline granules, and severe granular degeneration in the entire spinous and granular layers of the epidermis (**E**). Ultrastructurally, clumping of the keratin filaments *(arrows)* is seen within an upper epidermal keratinocyte (**F**).

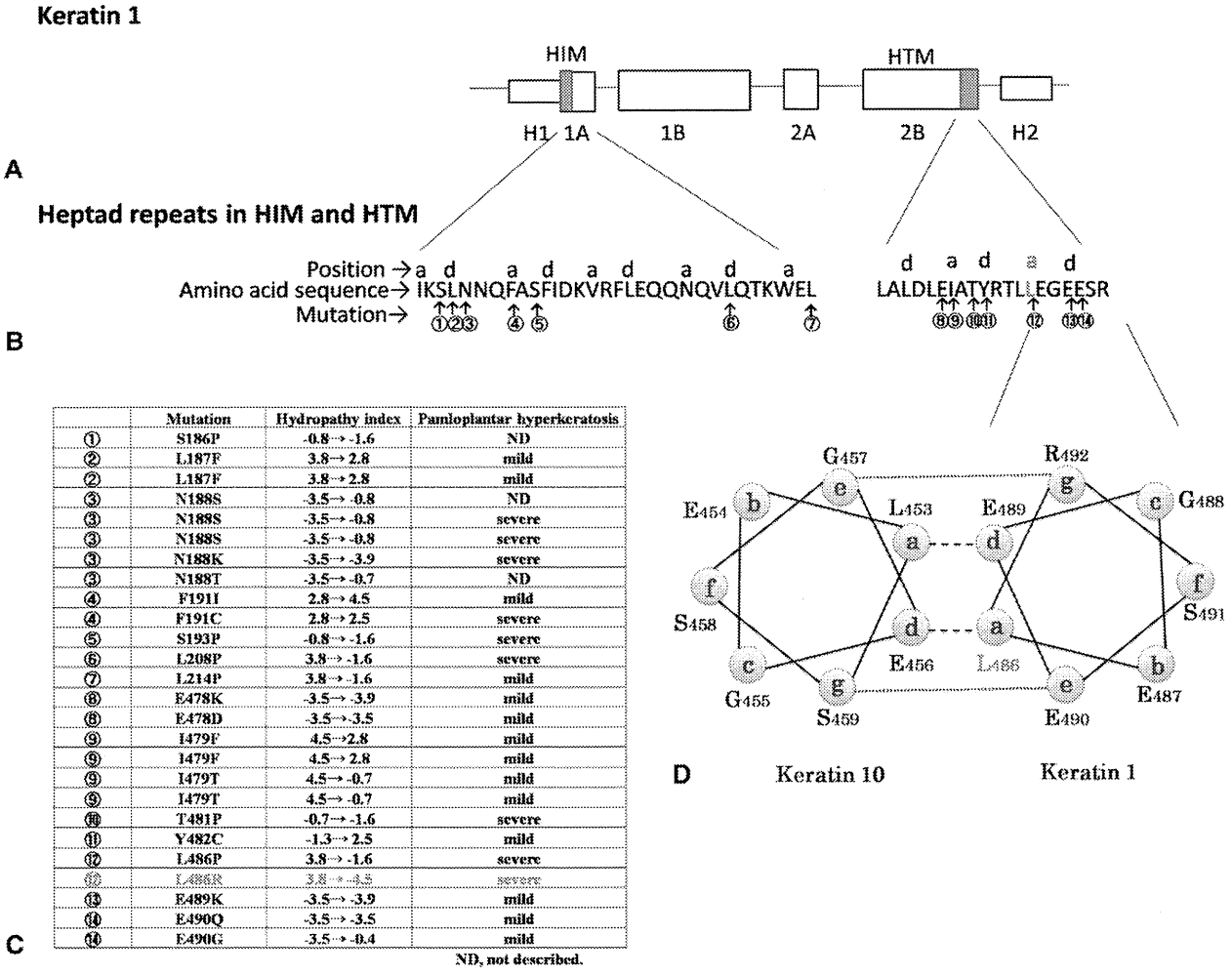

	Mutation	Hydropathy index	Palmoplantar hyperkeratosis
①	S186P	-0.8→-1.6	ND
②	L187F	3.8→2.8	mild
②	L187F	3.8→2.8	mild
③	N188S	-3.5→-0.8	ND
③	N188S	-3.5→-0.8	severe
③	N188S	-3.5→-0.8	severe
③	N188K	-3.5→-3.9	severe
③	N188T	-3.5→-0.7	ND
④	F191I	2.8→4.5	mild
④	F191C	2.8→2.5	severe
⑤	S193P	-0.8→-1.6	severe
⑥	L208P	3.8→-1.6	severe
⑦	L214P	3.8→-1.6	mild
⑧	E478K	-3.5→-3.9	mild
⑧	E478D	-3.5→-3.5	mild
⑨	I479F	4.5→2.8	mild
⑨	I479F	4.5→2.8	mild
⑨	I479T	4.5→-0.7	mild
⑨	I479T	4.5→-0.7	mild
⑩	T481P	-0.7→-1.6	severe
⑪	Y482C	-1.3→2.5	mild
⑫	L486P	3.8→-1.6	severe
⑫	L486R	3.8→-4.5	severe
⑬	E489K	-3.5→-3.9	mild
⑭	E490Q	-3.5→-3.5	mild
⑭	E490G	-3.5→-0.4	mild

ND, not described.

Fig 2. Summary of mutations in the helix initiation motif (HIM) and helix termination motif (HTM) of K1 from the Human Intermediate Filament Database (www.interfil.org/). **A**, Molecular structure of K1. **B**, Heptad repeats in HIM and HTM of K1 and mutation sites. The majority of cases (22 of 26) had mutations in the heptad repeat position *a, d, e,* and *g*. The present mutation is located at the *a* position leucine residue at codon no.486 *(red characters)* in the C-terminal—most heptad repeat. **C**, Summary of the *KRT1* mutations in HIM and HTM, alterations of hydropathy index, and levels of palmoplantar hyperkeratosis. Eight cases, including the present one, were reported as showing severe palmoplantar hyperkeratosis, and seven of those nine patients harbored mutations in the important *a, d, e,* and *g* position of heptad repeats. Mutations in this 486-leucine residue may seriously perturb the stability of keratin intermediate filaments. The substitution of arginine for leucine alters the character of the amino acid from that of a hydrophobic, apolar amino acid (hydropathy index of leucine, +3.8) to that of the most hydrophilic, basic amino acid (hydropathy index of arginine, −4.5). **D**, Heptad structure of the rod domain: schematic of a transverse cut through the last heptad (*abcdefg*) of the HTM of K1 and K10, showing hydrophobic interactions between positions *a* and *d (dashed lines)* and ionic hydrogen interactions between positions *e* and *g (dotted lines)*. Position *a* is occupied by apolar, hydrophobic amino acids. The *a* residues are thought to interact with amino acids located in the *d* position of the partner molecule of the heterodimer through hydrophobic interactions which stabilize the two-chain coiled-coil molecules. When the two strands coil around each other, positions *a* and *d* are internalized, stabilizing the structure, while positions *b, c, e, f,* and *g* are exposed on the surface of the protein. Residues at positions *e* and *g* stabilize dimer formation through ionic and hydrogen bonds.